



Developing Improved Optimization Algorithms for Ptychographic Image Reconstruction

Jaroslav Fowkes

STFC Computational Mathematics Group
Visiting Research Fellow at Oxford University

$$\begin{aligned}
\frac{D\underline{z}}{Dt} &= -\underline{\nabla} p + \mu \underline{\nabla}^2 \underline{z} + \frac{1}{S} \mu \underline{v} (\underline{v} \cdot \underline{z}) + \dots \\
\frac{Dp}{Dt} + \rho \underline{\nabla} \cdot \underline{z} &= 0 & -\underline{u} \cdot \underline{u}_3 &= \gamma_x \left(\frac{\partial u_i}{\partial x_j} + \frac{\partial u_j}{\partial x_i} \right) \\
p &= \rho RT & \frac{d(\rho_i)}{dt} + \underline{\nabla} \cdot (\rho_i \underline{z}) &= -\rho \underline{\nabla} \cdot \underline{z} + \dots
\end{aligned}$$

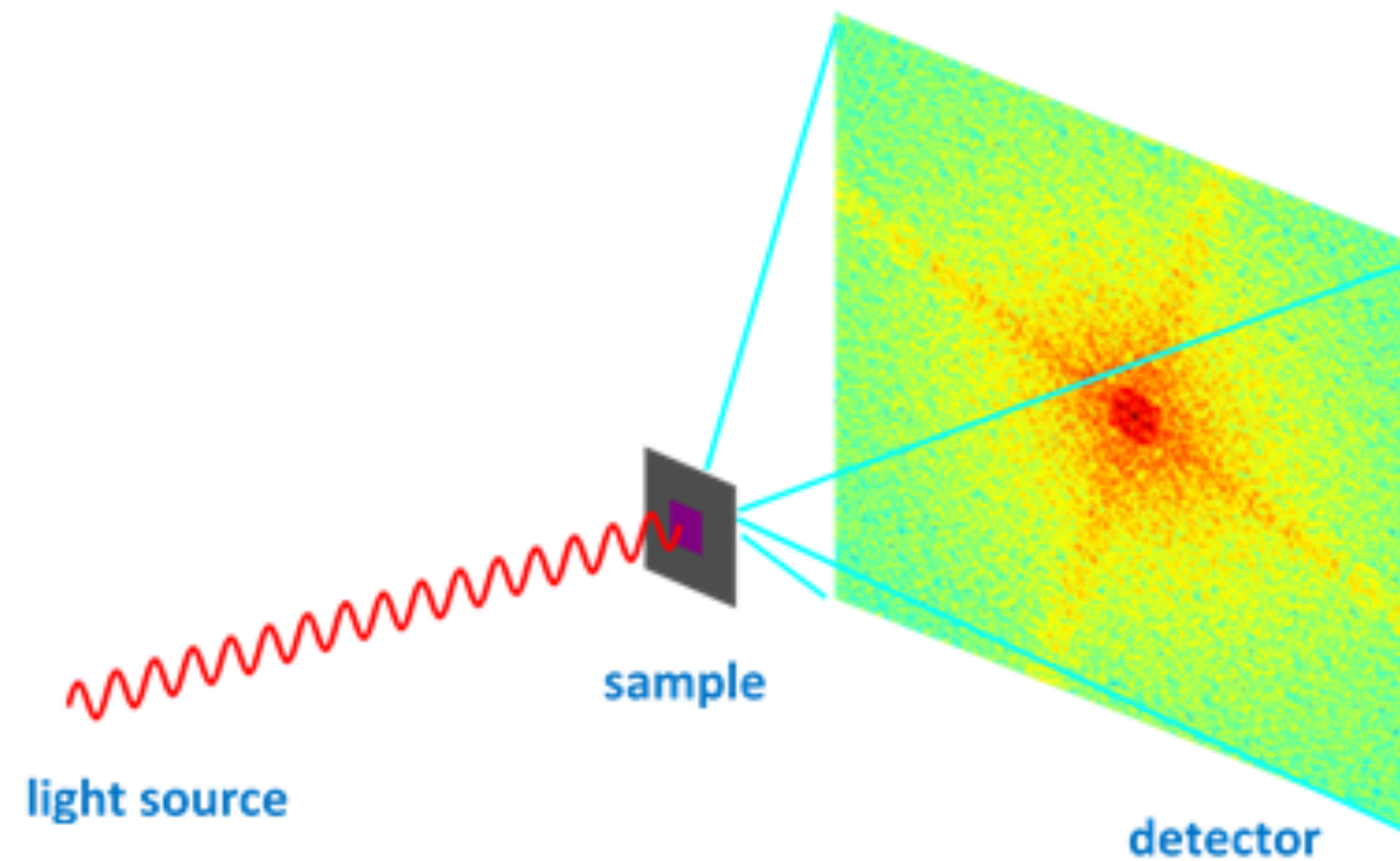
STFC Rutherford Appleton Laboratory



STFC manages the UK's major science facilities, at the Harwell campus we have:

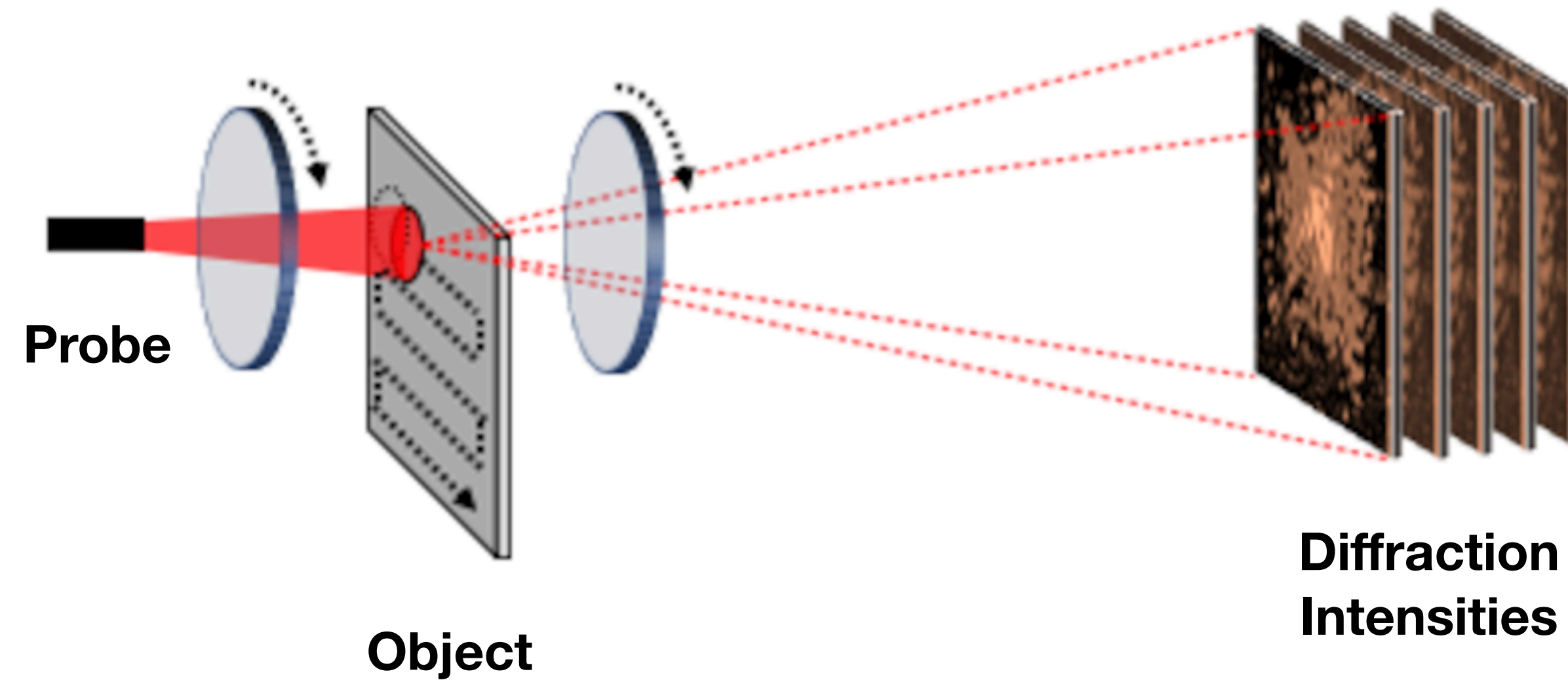
- Diamond Light Source
- Central Laser Facility
- ISIS Neutron Source
- RAL Space

Coherent Diffractive Imaging



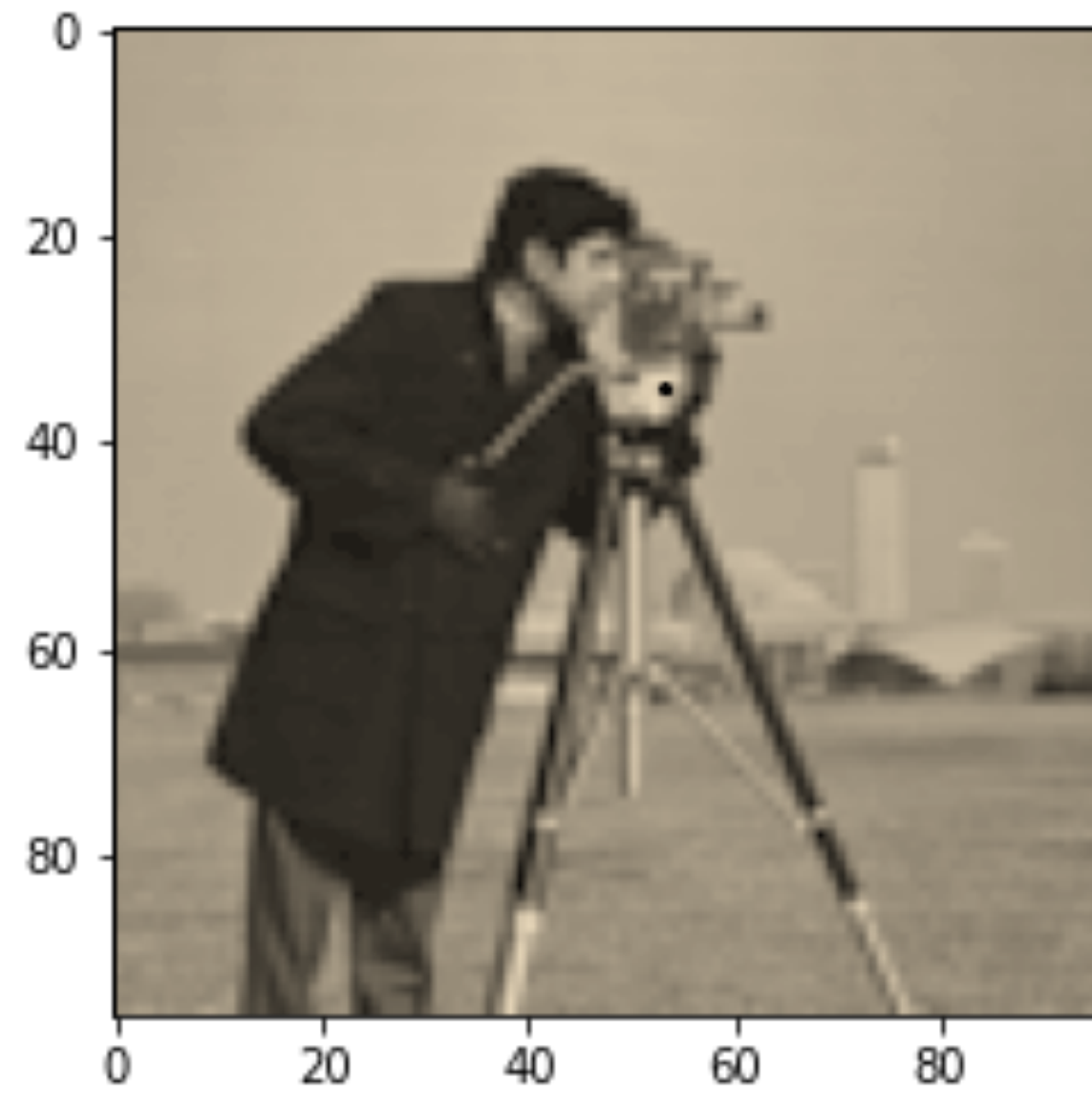
“CDI is a ‘lensless’ technique that allows imaging of matter at a spatial resolution not limited by lens aberrations. This technique exploits the measured diffraction pattern of a coherent beam scattered by an object to retrieve spatial information”

Ptychography

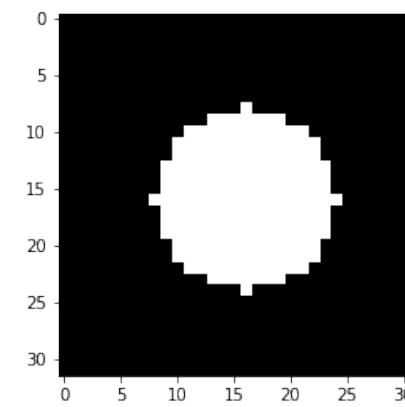


“Ptychography is an imaging technique in which a localized illumination scans overlapping regions of an object and generates a set of diffraction intensities used to computationally reconstruct its complex-valued transmission function”

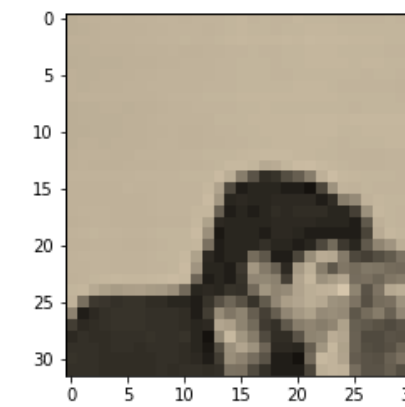
Exit Wave



$$o \in \mathbb{C}^{m \cdot m}$$



$$p \in \mathbb{C}^{n \cdot n}$$



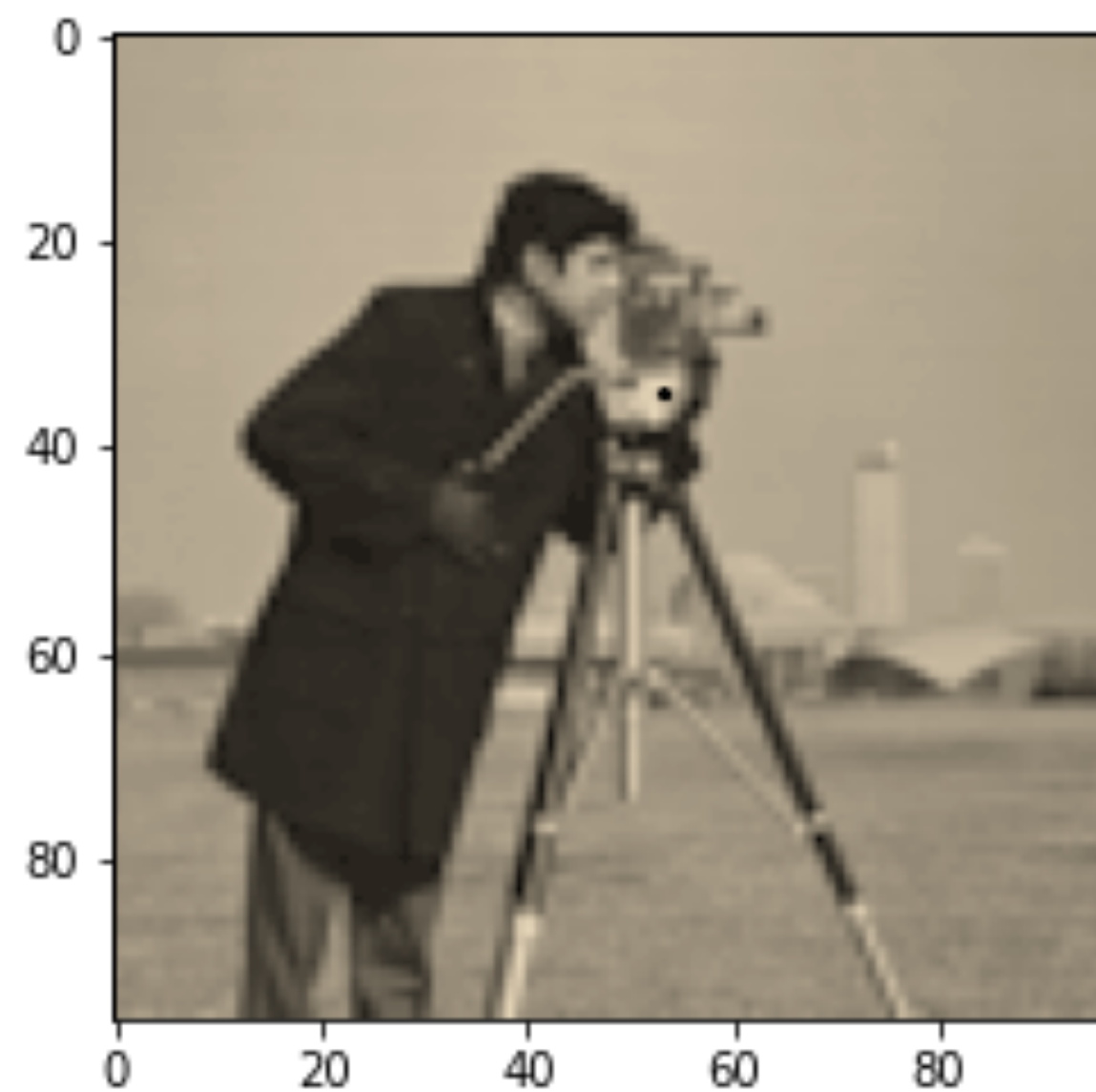
$$o_j \in \mathbb{C}^{n \cdot n}$$

Exit Wave:

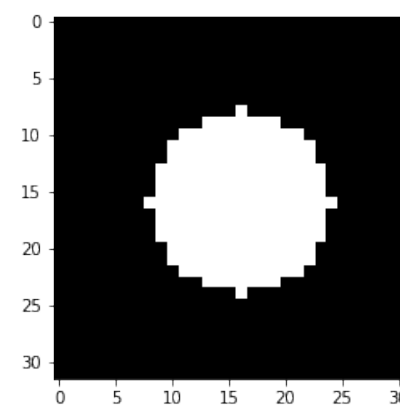
$$e_j = o_j p$$

by product we mean elementwise multiplication

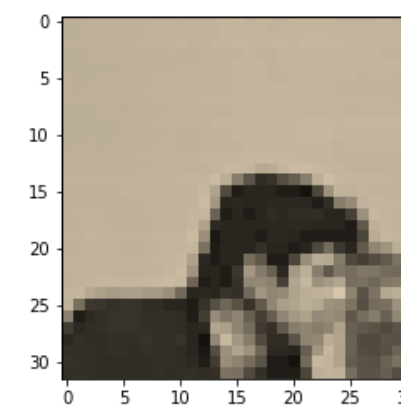
Wave Model



$$o \in \mathbb{C}^{m \cdot m}$$



$$p \in \mathbb{C}^{n \cdot n}$$



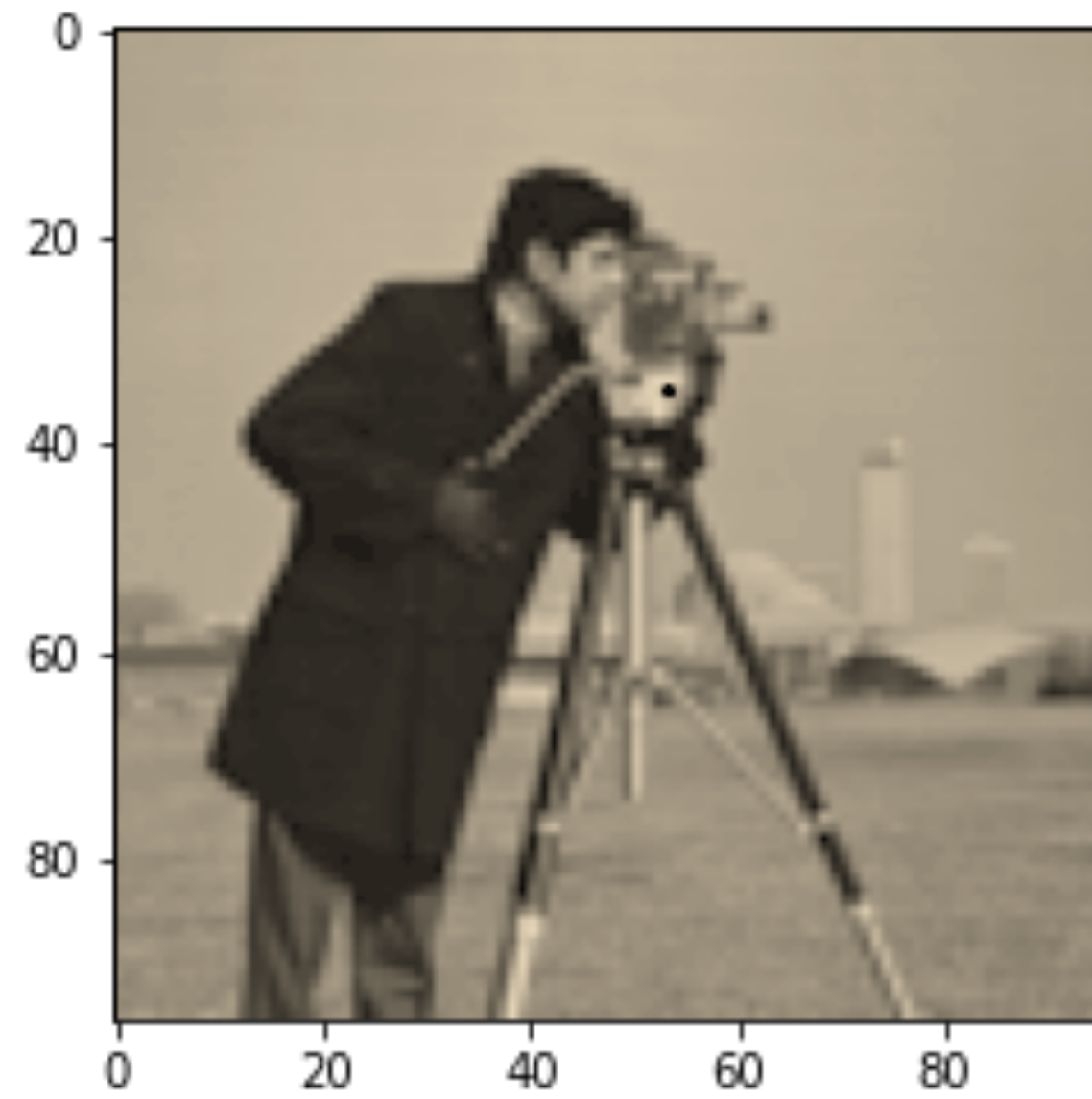
$$o_j \in \mathbb{C}^{n \cdot n}$$

Wave Model:

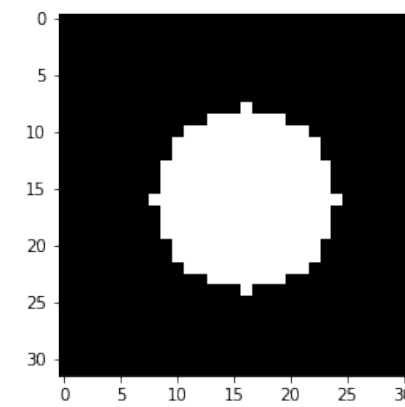
$$w_j = F(o_j p)$$

where F is the Discrete Fourier Transform (in 2D)

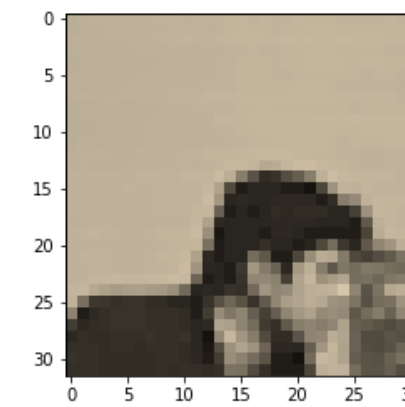
Forward Model



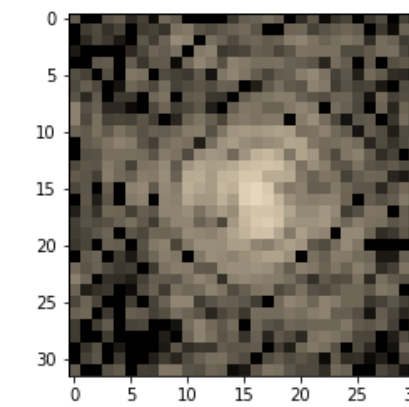
$$o \in \mathbb{C}^{m \cdot m}$$



$$p \in \mathbb{C}^{n \cdot n}$$



$$o_j \in \mathbb{C}^{n \cdot n}$$



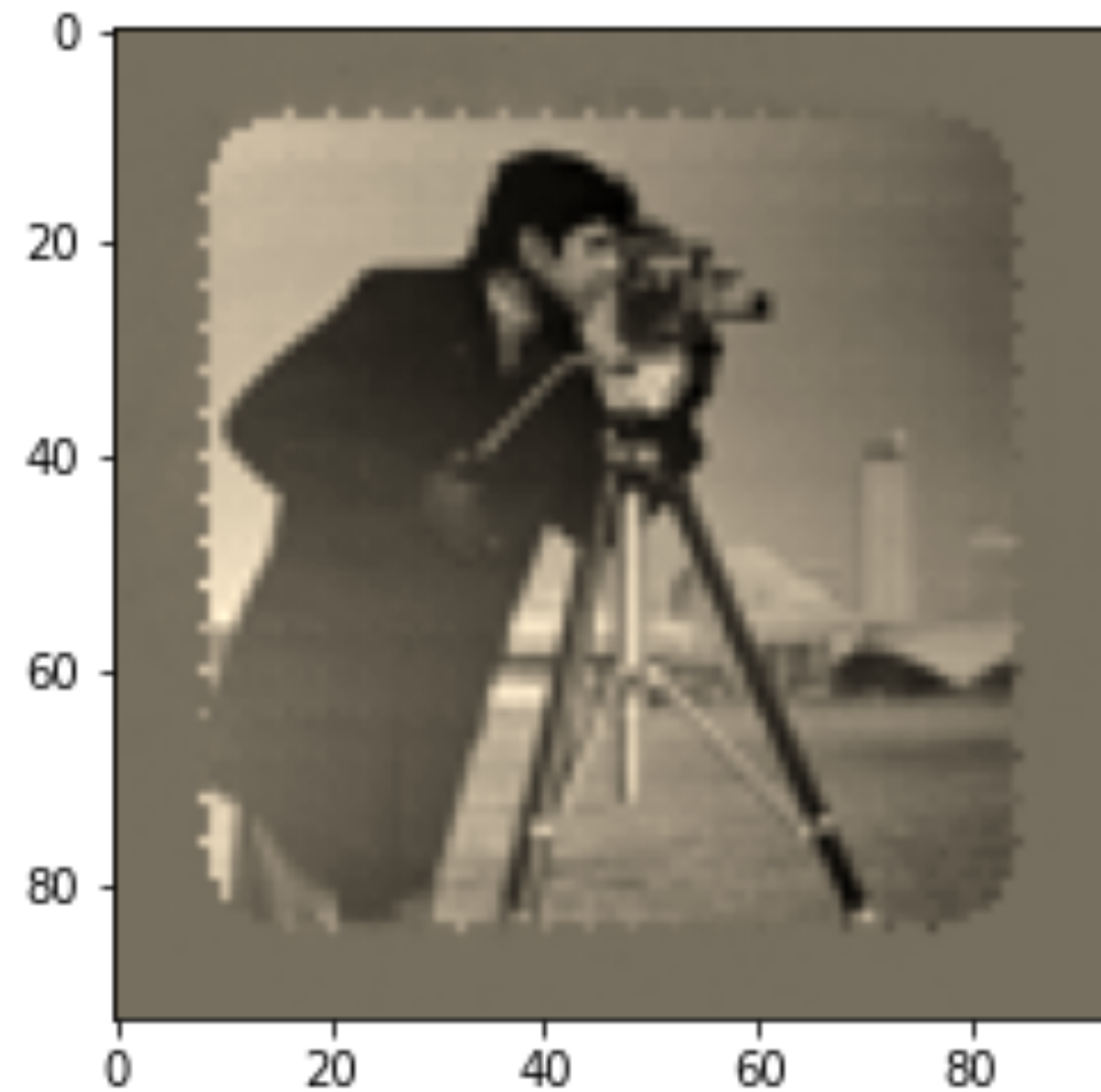
$$i_j \in \mathbb{R}^{n \cdot n}$$

Forward Model:

$$|w_j|^2 = |F(o_j p)|^2 \approx i_j$$

where F is the Discrete Fourier Transform (in 2D)

Reconstruction

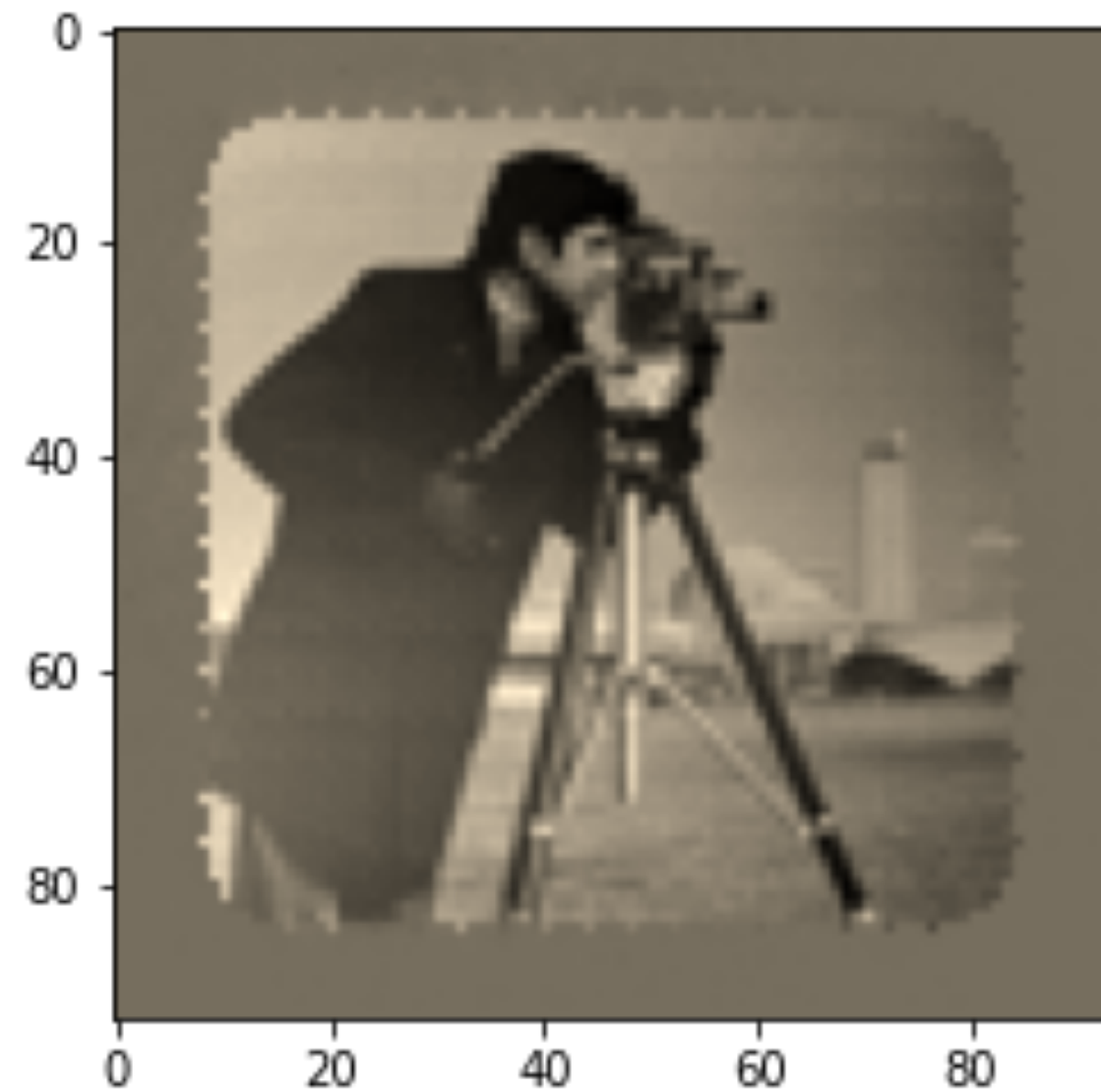


Reconstruct object (and probe) from measured intensities:

$$\min_{o_j p} \sum_j \left\| |F(o_j p)|^2 - i_j \right\|^2$$

The choice of error nom here is key (e.g. l^2 , likelihood, etc).

Inverse Problem



Reconstruct object (and probe) from measured intensities:

$$\min_{o_j p} \sum_j \left\| |F(o_j p)|^2 - i_j \right\|^2$$

a sum of nonlinear least-squares problems in $\mathbb{C}^{n \cdot n}$.

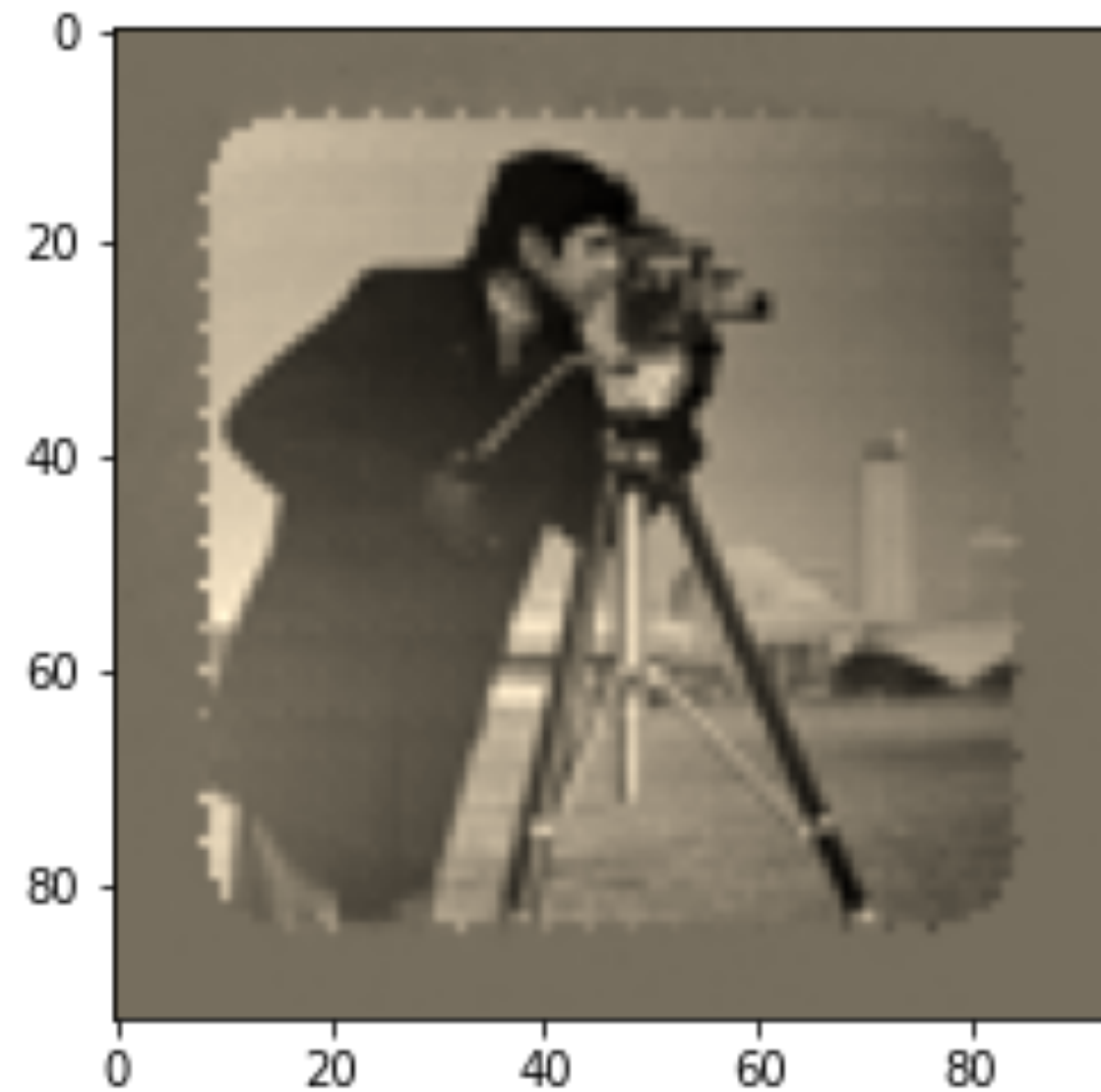
Inverse Problem

Unfortunately the inverse problem is not very well-posed, issues include:

- constant amplitude scaling: $o_j p = (A o_j) (A^{-1} p)$
- constant phase offset: $o_j p = (e^{i\phi} o_j) (e^{-i\phi} p)$
- global probe and object translation
- linear phase ramp (i.e. DFT shift theorem)

However most of these issues can be addressed with suitable constraints.

Nonlinear least-squares

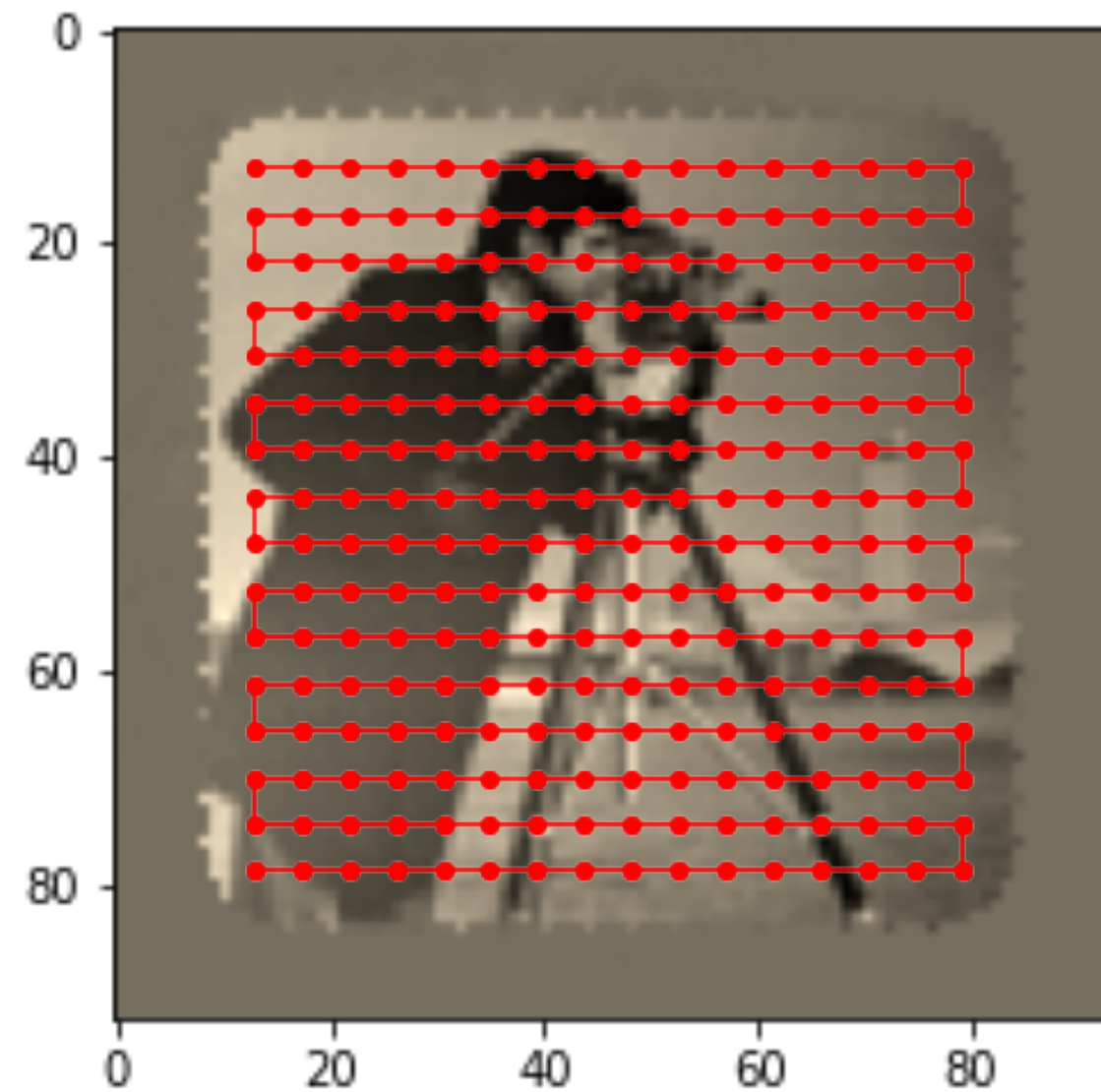


Reconstruct object (and probe) from measured intensities:

$$\min_{o_j p} \sum_j \left\| |F(o_j p)|^2 - i_j \right\|^2$$

a sum of nonlinear least-squares problems in $\mathbb{C}^{n \cdot n}$.

Nonlinear least-squares



Reconstruct object (and probe) from measured intensities:

$$\min_{o_j p} \sum_j \left\| |F(o_j p)|^2 - i_j \right\|^2$$

a sum of nonlinear least-squares problems in $\mathbb{C}^{n \cdot n}$.

Nonlinear least-squares

Given a nonlinear least-squares problem

$$f(x) = \|r(x)\|^2$$

with nonlinear residual $r: \mathbb{R}^n \rightarrow \mathbb{R}^m$, the gradient is given by

$$\nabla f(x) = 2J(x)^T r(x)$$

where $J(x) = [\partial r_i / \partial x_j]_{ij}$ is the Jacobian matrix, and the Hessian is given by

$$\nabla^2 f(x) = 2J(x)^T J(x) + 2 \sum_i r_i(x) \nabla^2 r_i(x)$$

However, often in practice the Hessian is too expensive to compute.

Gauss-Newton approximation

The first order optimality conditions for unconstrained optimization are:

$$\nabla f(x) = 0$$

applying Newton's method to this equation gives the step s^k from x^k as

$$\nabla^2 f(x^k) s^k = - \nabla f(x^k)$$

The idea behind Gauss-Newton is to use the approximation

$$\nabla^2 f(x^k) \approx 2J^T(x^k)J(x^k) + 2 \sum_i r_i(x^k) \nabla^2 r_i(x^k)$$

In particular this is asymptotically exact for zero residual problems.

L-BFGS Approximation

A BFGS step approximates the Hessian with the matrix B^k

$$s^{k+1} = - (B^{k+1})^{-1} \nabla f(x^{k+1})$$

using past gradients $y^k = \nabla f(x^{k+1}) - \nabla f(x^k)$ as the rank-2 update

$$B^{k+1^{-1}} = \left(I - \frac{s^k y^k T}{y^k T s^k} \right) B^{k^{-1}} \left(I - \frac{y^k s^k T}{y^k T s^k} \right) + \frac{s^k s^k T}{y^k T s^k}$$

L-BFGS only uses a fixed number (limited memory) of past s^k, y^k .

BFGS



Broyden, Fletcher, Goldfarb, Shanno

Nonlinear CG

Nonlinear CG is a generalisation of CG to general nonlinear objectives.

Starting from the steepest descent direction

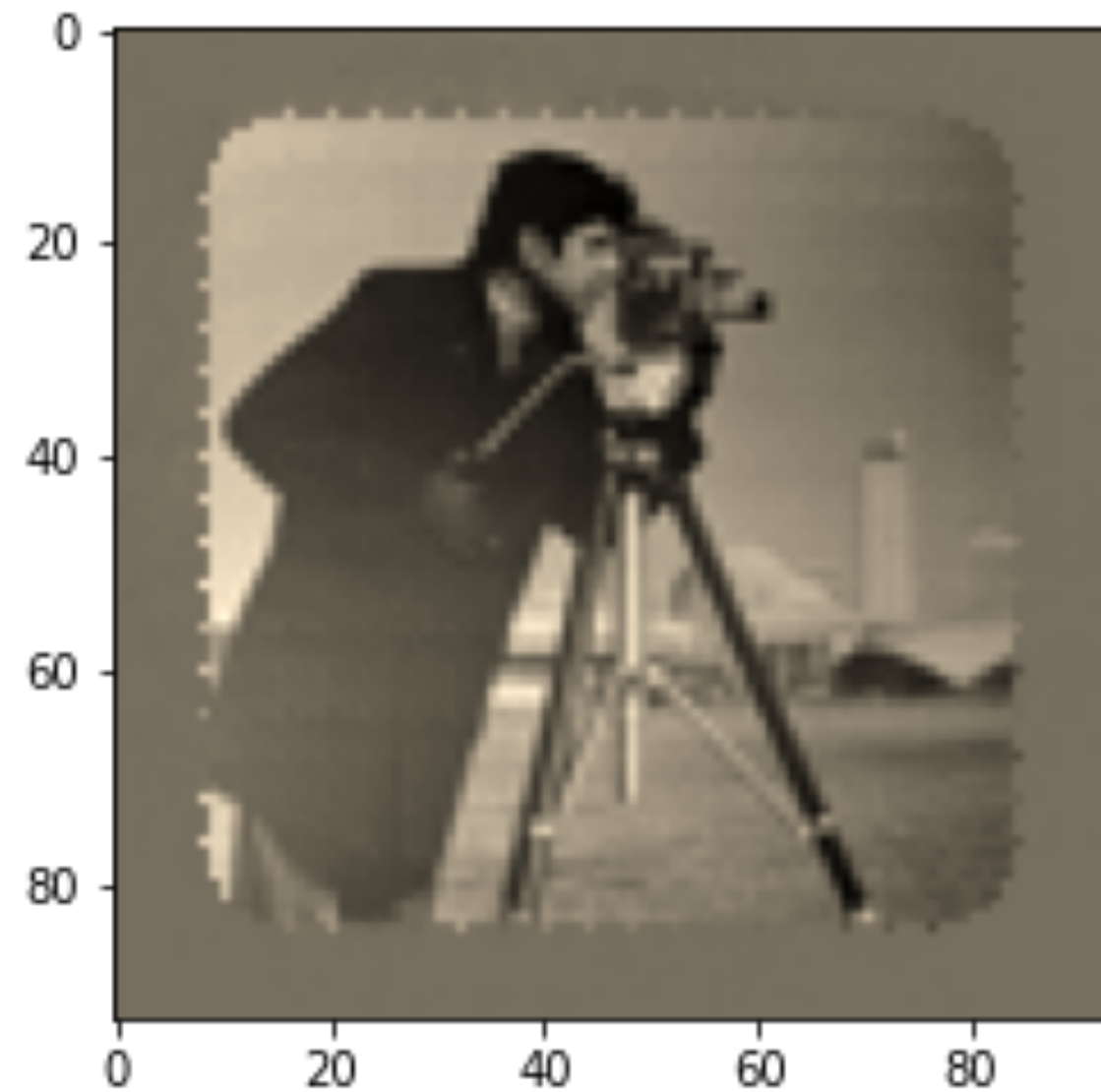
$$s^0 = -\nabla f(x^0)$$

nonlinear CG proceeds along the approximately conjugate directions

$$s^{k+1} = -\nabla f(x^{k+1}) + \beta^k s^k$$
$$\beta^k = \frac{\|\nabla f(x^{k+1})\|^2}{\|\nabla f(x^k)\|^2}$$

Many choices of β^k are possible here (Fletcher-Reeves, Polak-Ribière, etc).

Optimization: least-squares



Notice that the objective is not analytic (due to the modulus):

$$\min_{o_j p} \sum_j \left\| |F(o_j p)|^2 - i_j \right\|^2$$

hence can only optimize it by identifying $\mathbb{C} \cong \mathbb{R} \times \mathbb{R}$.

Wirtinger Derivatives

Wirtinger derivatives neatly extend complex derivatives to $\mathbb{C} \cong \mathbb{R} \times \mathbb{R}$, for $z = x + iy \in \mathbb{C}$ define:

$$\frac{\partial}{\partial z} = \frac{1}{2} \left(\frac{\partial}{\partial x} - i \frac{\partial}{\partial y} \right)$$
$$\frac{\partial}{\partial z^*} = \frac{1}{2} \left(\frac{\partial}{\partial x} + i \frac{\partial}{\partial y} \right)$$

where z^* denotes complex conjugation. To convert to (x, y) -space derivatives we can then use:

$$\frac{\partial}{\partial x} + i \frac{\partial}{\partial y} = 2 \left(\frac{\partial}{\partial z} \right)^*$$

For analytic functions the complex derivative agrees with the first Wirtinger derivative (the second is zero).

Wirtinger Calculus

For example, for the modulus function:

$$s(z) = |z|^2 = x^2 + y^2$$

we have that

$$\frac{\partial s}{\partial x} = 2x \quad \frac{\partial s}{\partial y} = 2y$$

and therefore that

$$\frac{\partial s}{\partial z} = x - iy = z^*$$
$$\frac{\partial s}{\partial z^*} = x + iy = z$$

And for the product function:

$$m(z_1, z_2) = z_1 z_2 = x_1 x_2 + i(x_1 y_2 + x_2 y_1) - y_1 y_2$$

we have that

$$\frac{\partial m}{\partial x_1} = x_2 + iy_2 \quad \frac{\partial m}{\partial y_1} = ix_2 - y_2$$

and therefore that

$$\frac{\partial s}{\partial z_1} = x_2 + iy_2 = z_2$$
$$\frac{\partial s}{\partial z_1^*} = 0$$

Nonlinear Least-squares

Consider the objective for j th scan position:

$$f_j(o_j, p) = \| r_j \|^2 = \left\| |w_j|^2 - i_j \right\|^2$$

where $w_j = F(o_j, p)$ is the wave model. Then:

$$\nabla_{o_j} f_j = 2J_{o_j}^T r_j = 4F^{-1} \left(w_j r_j \right) p^*$$

$$\nabla_p f_j = 2J_p^T r_j = 4F^{-1} \left(w_j r_j \right) o_j^*$$

are the gradients when viewing $\mathbb{C} \cong \mathbb{R} \times \mathbb{R}$

Gauss-Newton

Approximates Hessian matrix using only first-order terms:

$$\nabla^2 f_j \approx 2 \begin{pmatrix} J_{o_j}^T J_{o_j} & J_{o_j}^T J_p \\ J_p^T J_{o_j} & J_p^T J_p \end{pmatrix}$$

where J are Jacobians. Too big to form, consider Hessian-vector products:

$$\nabla^2 f_j \begin{pmatrix} v_{o_j} \\ v_p \end{pmatrix} \approx 8 \begin{pmatrix} p^* F^{-1} \left(w_j^2 F^{-1}(p^* v_{o_j}) \right) + p^* F^{-1} \left(w_j^2 F^{-1}(o_j^* v_p) \right) \\ o_j^* F^{-1} \left(w_j^2 F^{-1}(p^* v_{o_j}) \right) + o_j^* F^{-1} \left(w_j^2 F^{-1}(o_j^* v_p) \right) \end{pmatrix}$$

unfortunately these turn out to be extremely ill-conditioned.

L-BFGS

L-BFGS steps use approximate object and probe Hessians

$$s_o^{k+1} = - \sum_j (B_{o_j}^{k+1})^{-1} \nabla_{o_j} f_j^{k+1}$$

$$s_p^{k+1} = - \sum_j (B_p^{k+1})^{-1} \nabla_p f_j^{k+1}$$

calculated using a two-loop recursion for the BFGS formula:

$$B^{k+1^{-1}} = \left(I - \frac{s^k y^{kT}}{y^{kT} s^k} \right) B^{k^{-1}} \left(I - \frac{y^k s^{kT}}{y^{kT} s^k} \right) + \frac{s^k s^{kT}}{y^{kT} s^k}$$

which is computationally much more efficient.

Nonlinear CG

Proceed along conjugate directions, starting from steepest descent:

$$s_o^0 = - \sum_j \nabla_{o_j} f_j = - \sum_j 4F^{-1} \left(w_j r_j \right) p^*$$

$$s_p^0 = - \sum_j \nabla_p f_j = - \sum_j 4F^{-1} \left(w_j r_j \right) o_j^*$$

and updating the directions in the standard way (with suitable β):

$$s_o^{k+1} = - \sum_j \nabla_{o_j} f_j^{k+1} + \beta^k s_o^k$$

$$s_p^{k+1} = - \sum_j \nabla_p f_j^{k+1} + \beta^k s_p^k$$

$$\beta^k = \frac{\sum_j \|\nabla_{o_j} f_j^{k+1}\|^2 + \|\nabla_p f_j^{k+1}\|^2}{\sum_j \|\nabla_{o_j} f_j^k\|^2 + \|\nabla_p f_j^k\|^2}$$

Exact Linesearch

Taking object and probe steps with step-size α :

$$o_j(\alpha) = o_j + \alpha s_o$$

$$p(\alpha) = p + \alpha s_p$$

and substituting into objective for j th scan position gives

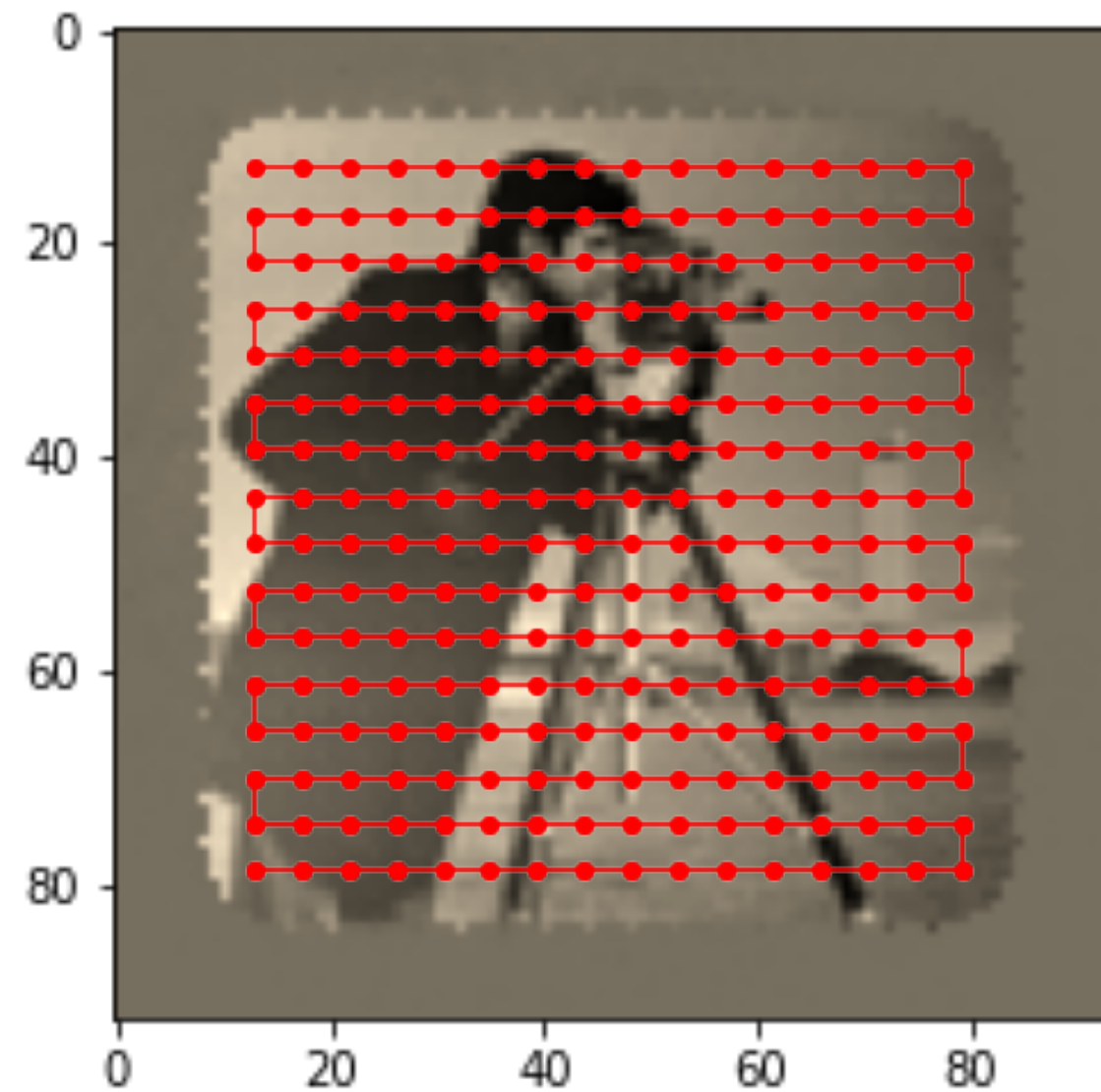
$$f_j(o_j(\alpha), p(\alpha)) = \left\| |F(o_j(\alpha)p(\alpha))|^2 - i_j \right\|^2 = \left(\sum_{n=0}^4 c_n \alpha^n \right)^2$$

Thus to find the optimal step length we can solve

$$0 = \sum_j \nabla_{\alpha} f_j(o_j(\alpha), p(\alpha)) = \sum_j \left(\sum_{n=1}^4 n c_n \alpha^{n-1} \right)^2$$

by finding the smallest real root of this real polynomial.

ePIE Algorithm



ePIE algorithm considers more natural amplitude objective:

$$\min_{o_j p} \sum_j \left\| |F(o_j p)| - \sqrt{i_j} \right\|^2$$

and performs *for each j at random* a two-stage optimization.

Fourier and Real Spaces

All ptychography algorithms have to satisfy two constraints

Firstly, the modulus constraint in Fourier space:

$$|F(e_j)| = \sqrt{i_j}$$

Secondly, the overlap constraint in real space:

$$e_j = o_j p$$

which is enforced for all j scan positions.

ePIE Algorithm

First, consider amplitude objective for j th scan position:

$$f_j(w_j) = \left\| |w_j| - \sqrt{i_j} \right\|^2$$

where $w_j = F(o_j p)$ and perform a wave model update:

$$w_j^{k+1} = w_j^k - \alpha_j \nabla_{w_j} f_j$$

Second, consider the difference between exit waves:

$$g_j(o_j, p) = \left\| o_j p - F^{-1}(w_j^{k+1}) \right\|^2$$

and perform a steepest descent update wrt o_j, p .

ePIE Algorithm

First update is equivalent to the modulus constraint:

$$\hat{e}_j = F^{-1} \left(\sqrt{i_j} \exp(i \text{Arg}[w_j]) \right)$$

where \hat{e}_j is the exit wave $o_j p$ with replaced modulus.

Second update takes a step along the gradients of g_j :

$$\nabla_{o_j} g_j = 2 \left(o_j p - \hat{e}_j \right) p^*$$

$$\nabla_p g_j = 2 \left(o_j p - \hat{e}_j \right) o_j^*$$

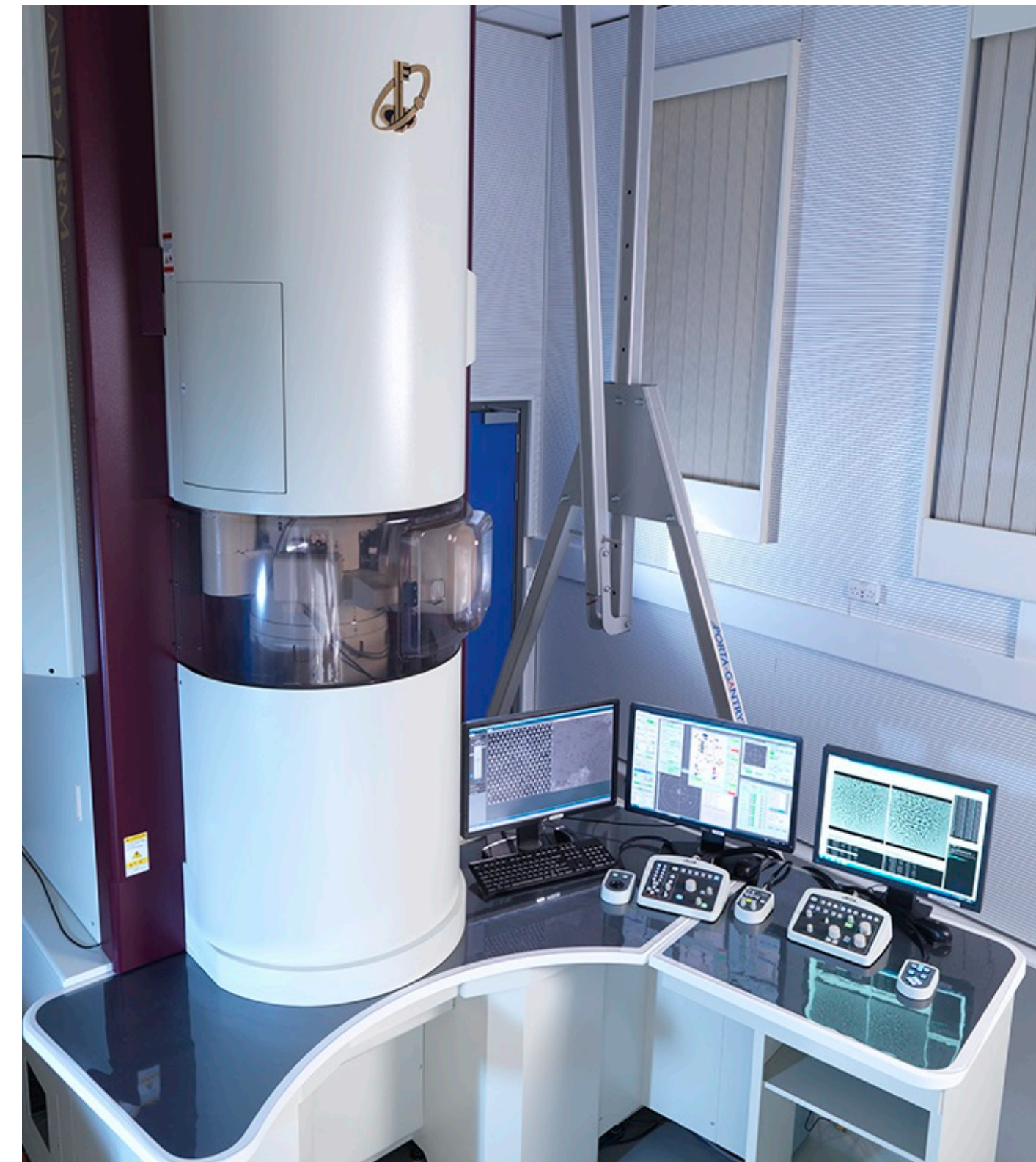
with step-sizes $1/2|p|_{\max}^2$ and $1/2|o_j|_{\max}^2$ respectively.

Example: ePSIC

electron Physical Science Imaging Centre



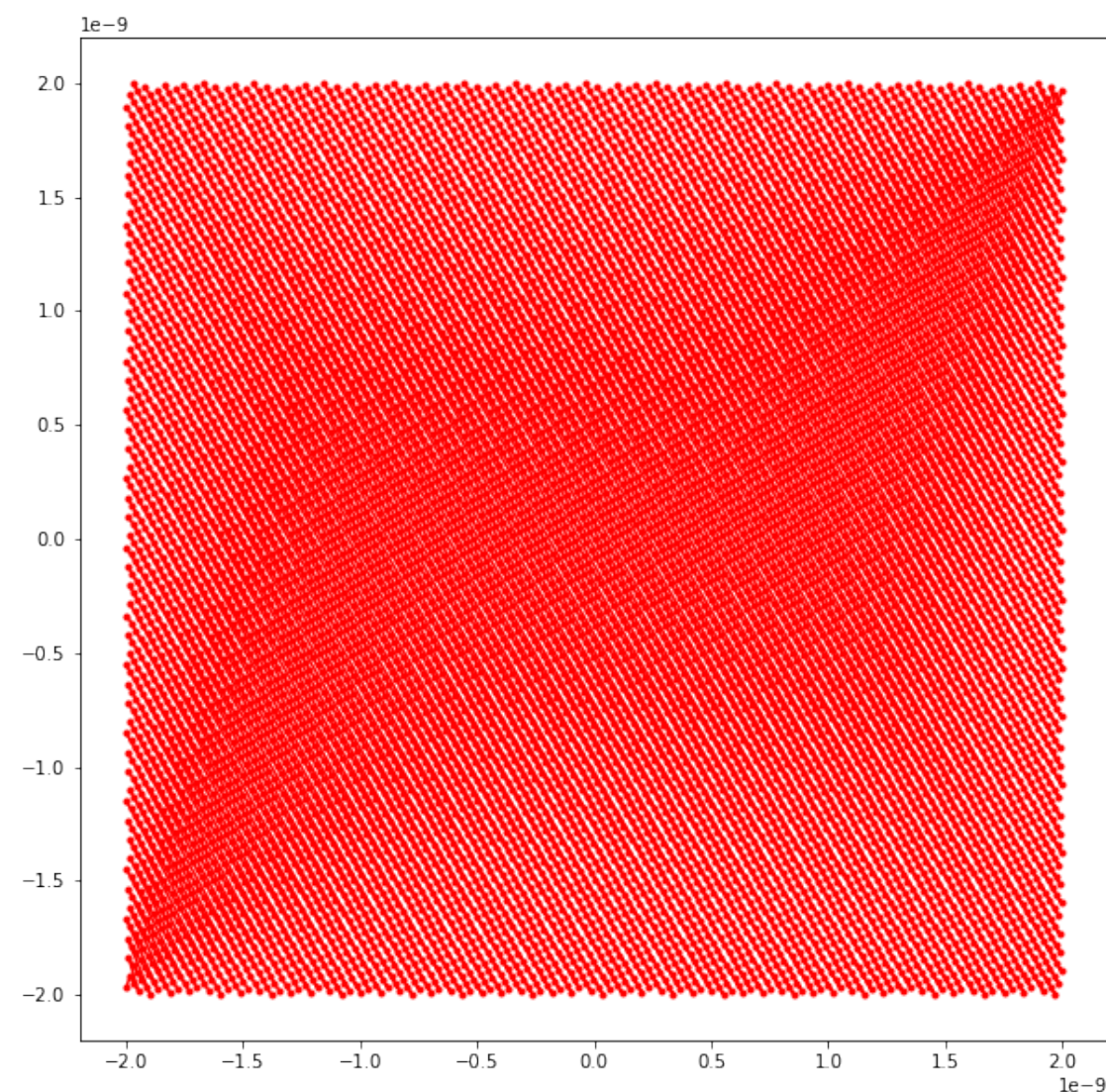
JEOL ARM200F



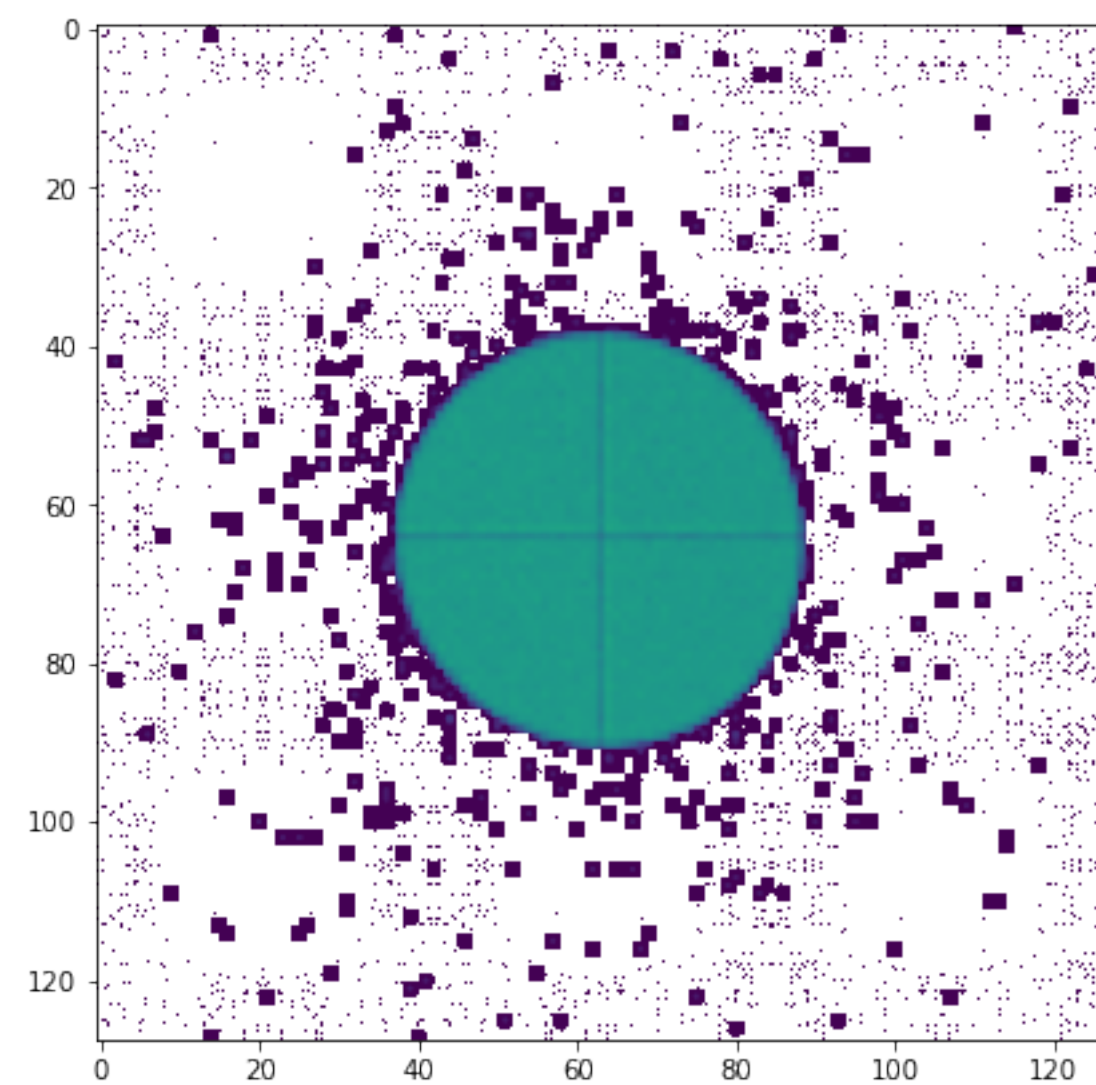
JEOL ARM300F

Example: Graphene Layers

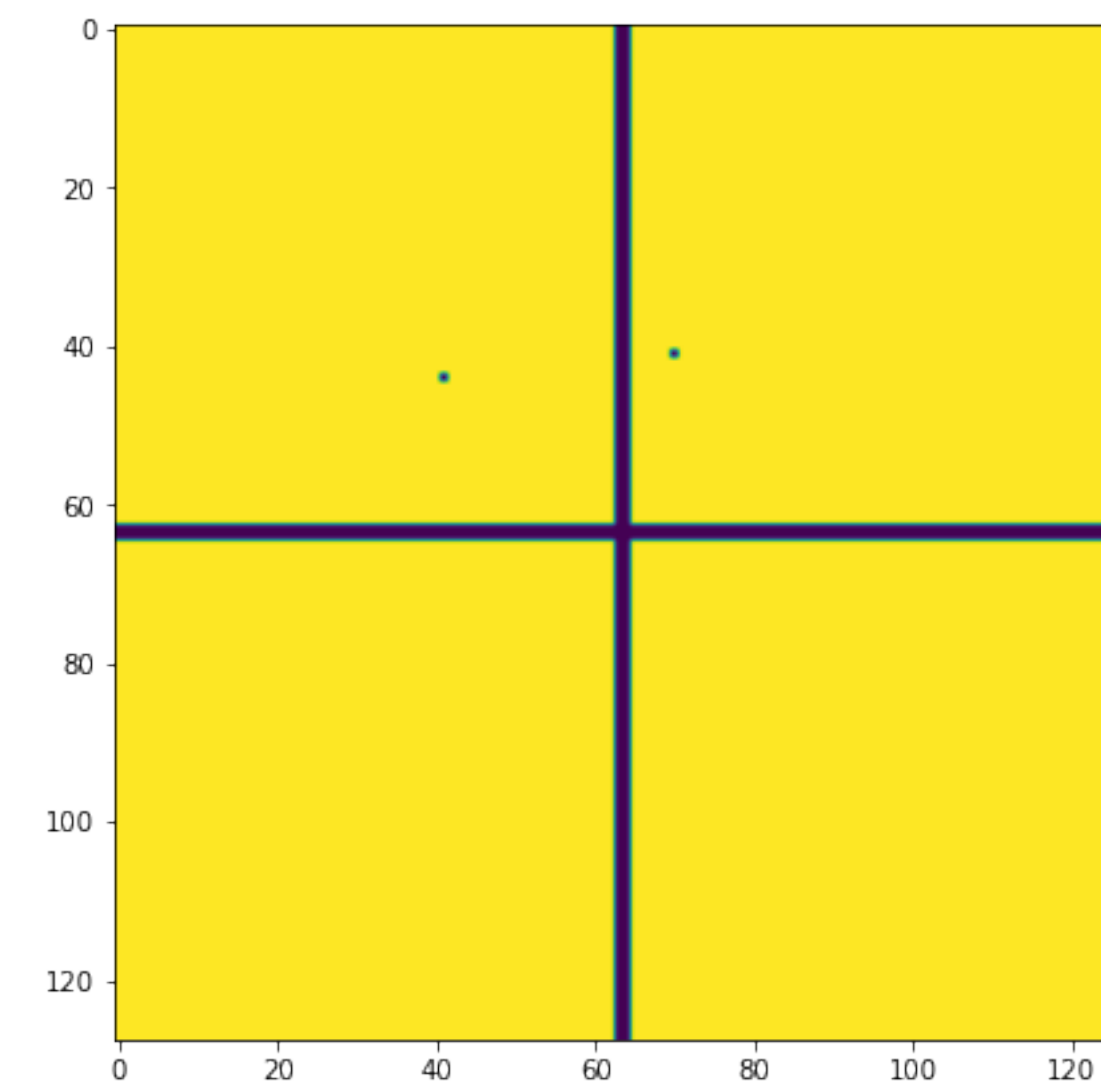
Graphene dataset courtesy of Chris Allen (ePSIC)



Scan
Positions



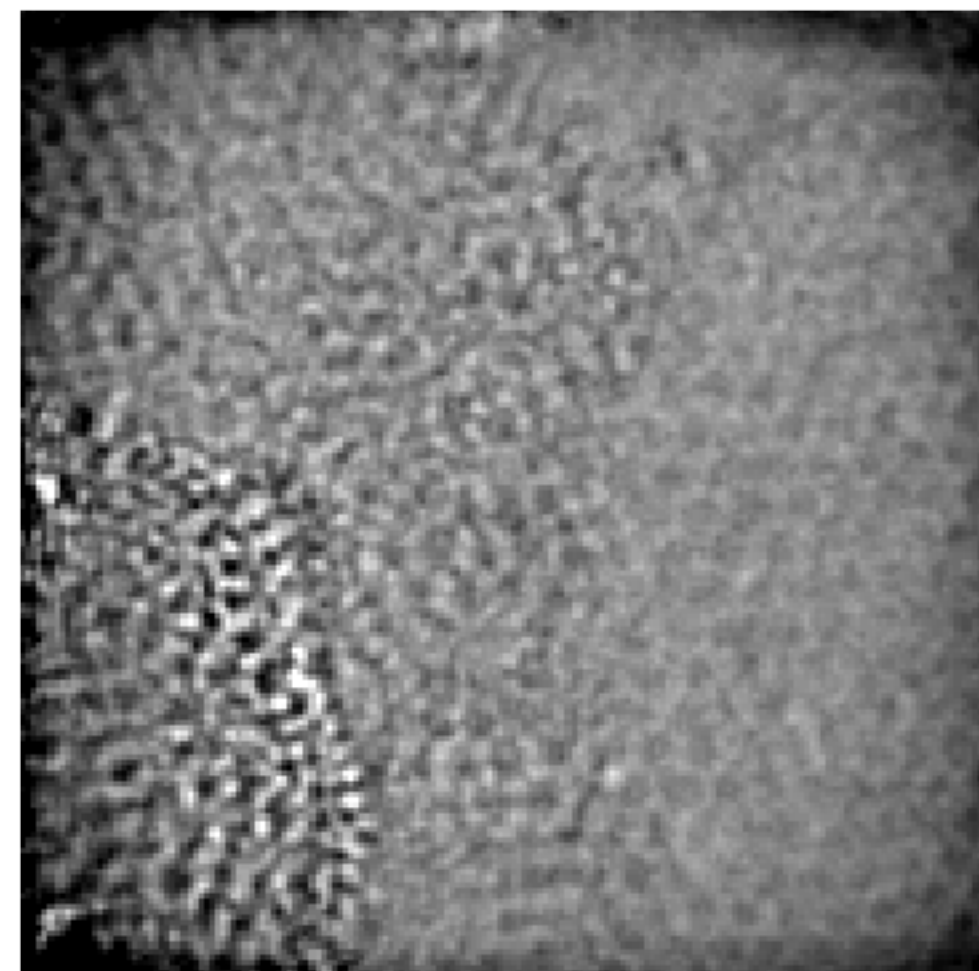
Diffraction
Intensity



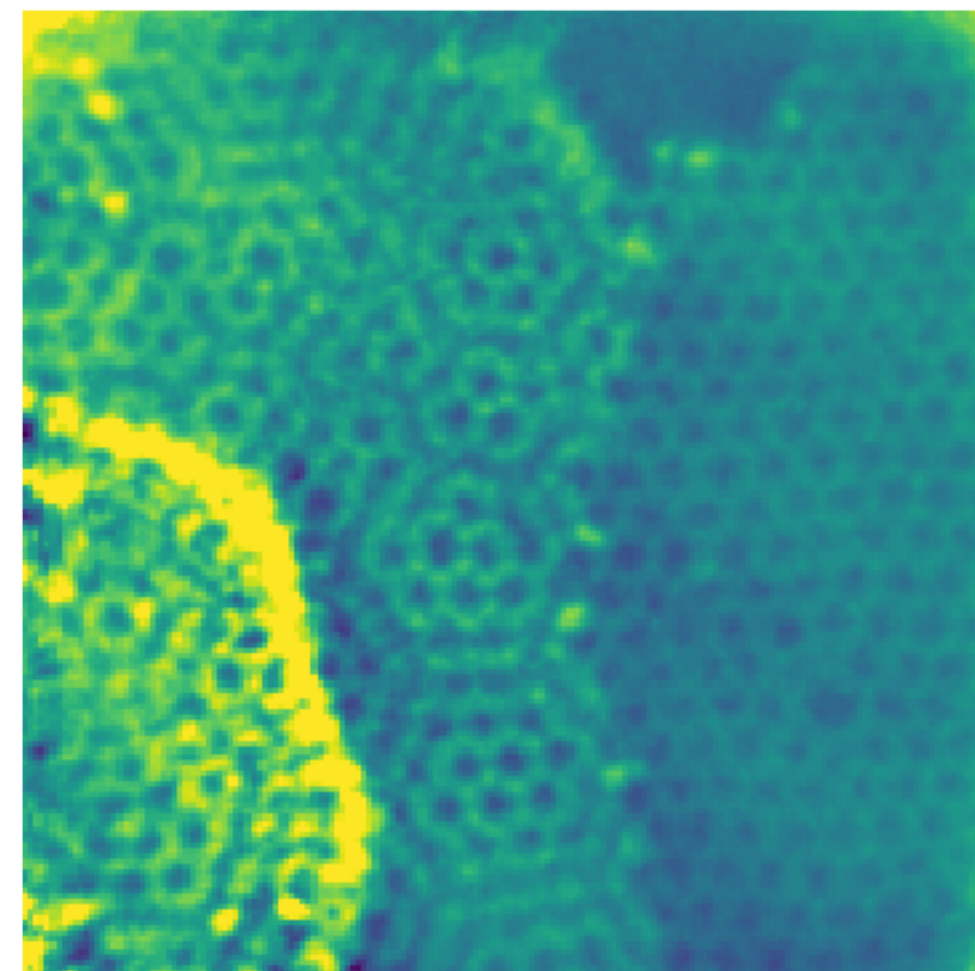
Detector
Mask

Example: ePIE

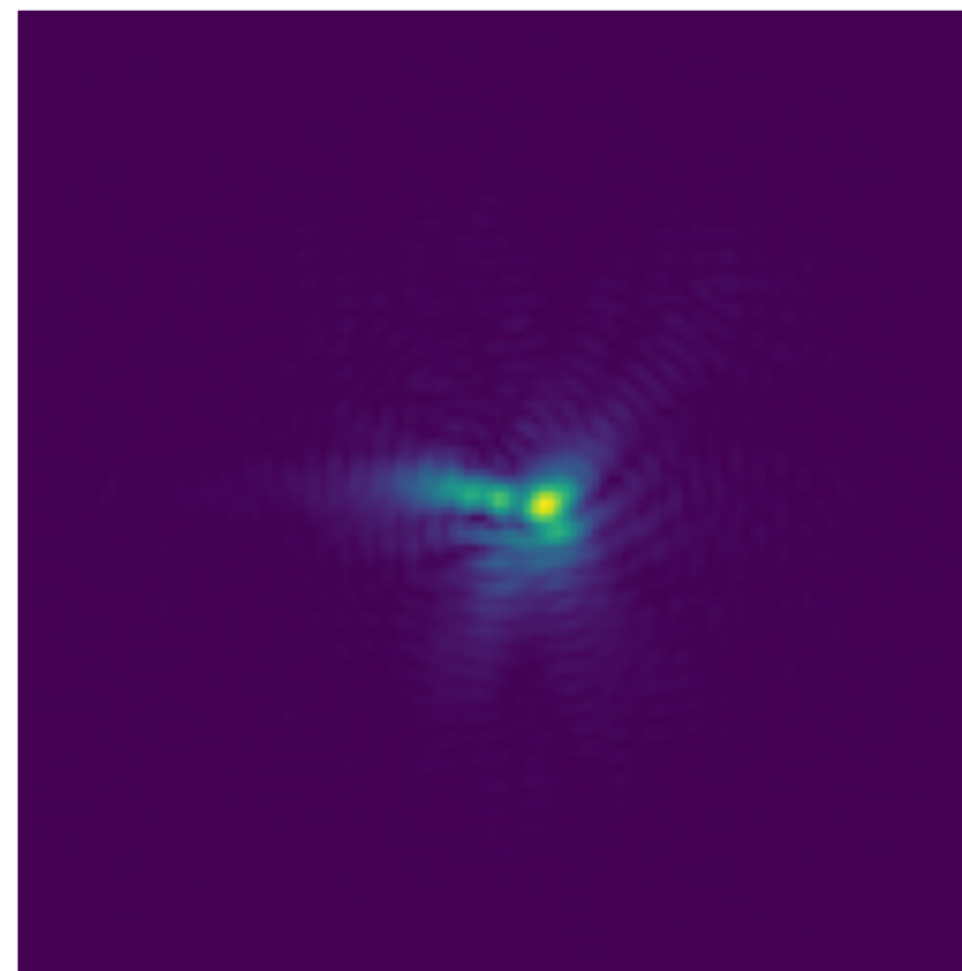
Graphene dataset courtesy of Chris Allen (ePSIC)



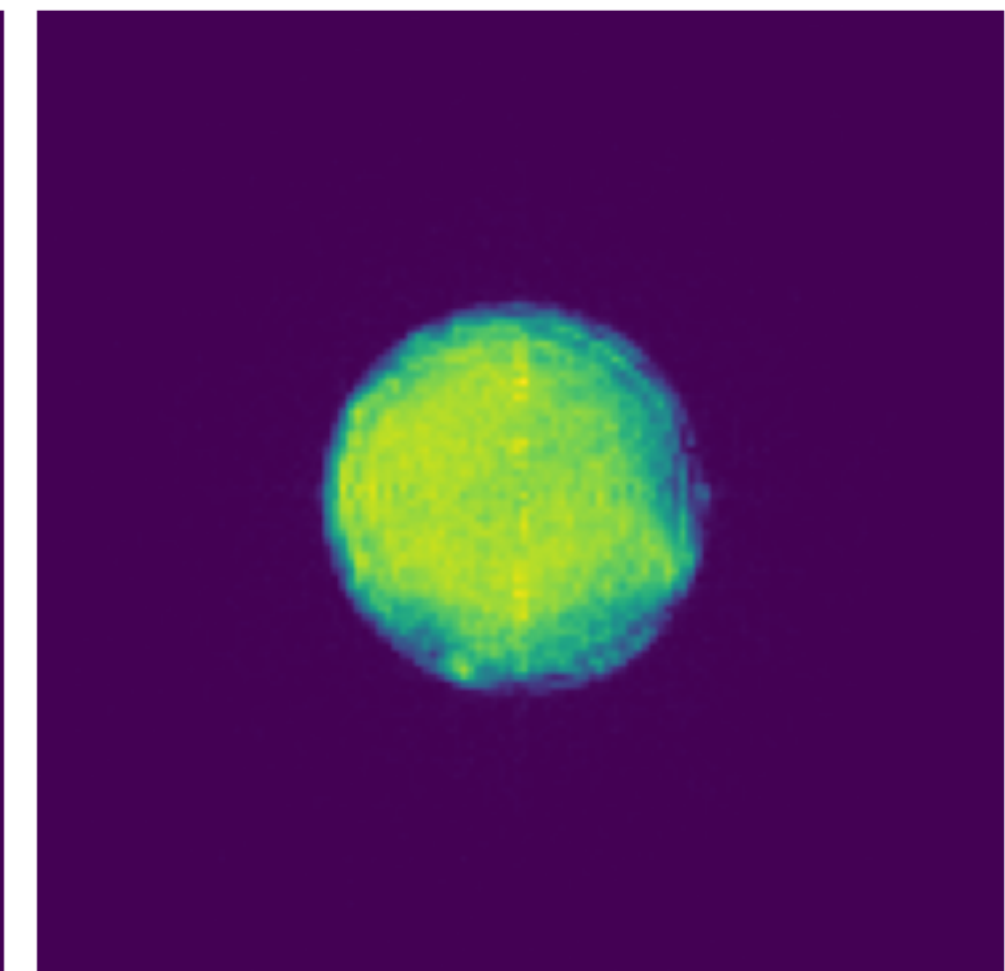
Object Amplitude



Object Phase



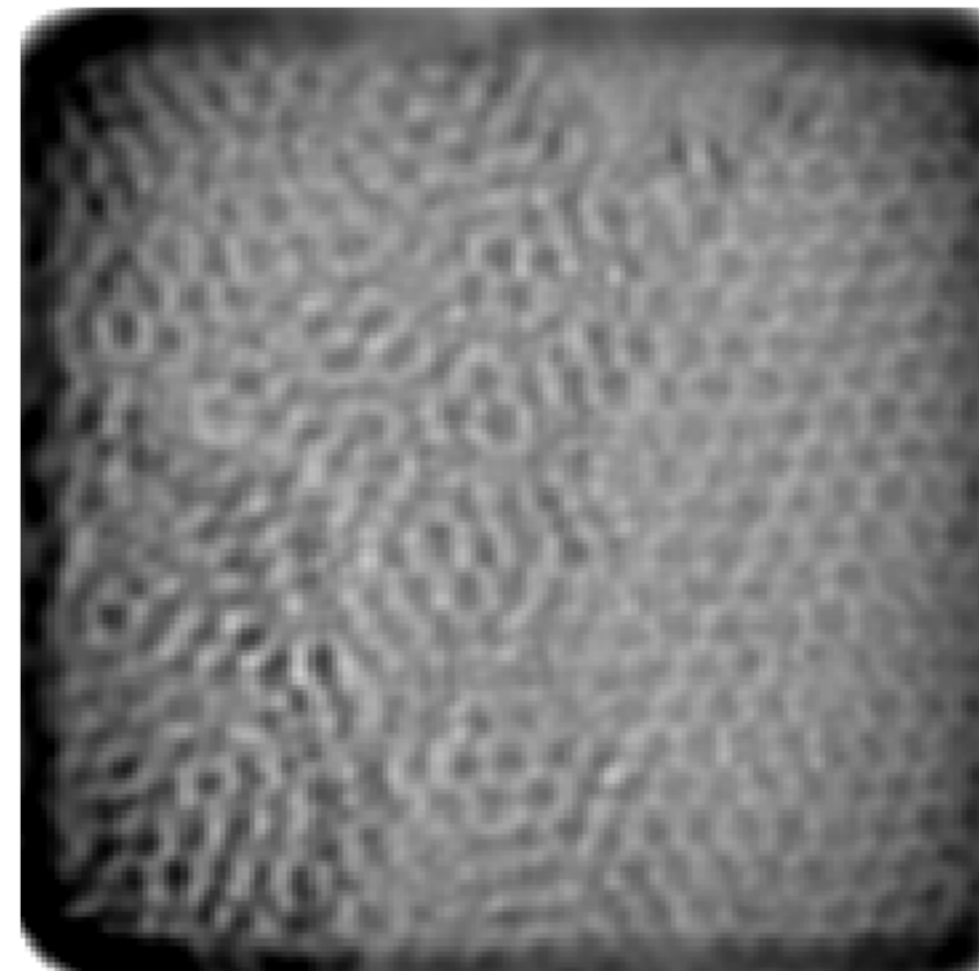
Probe Amplitude



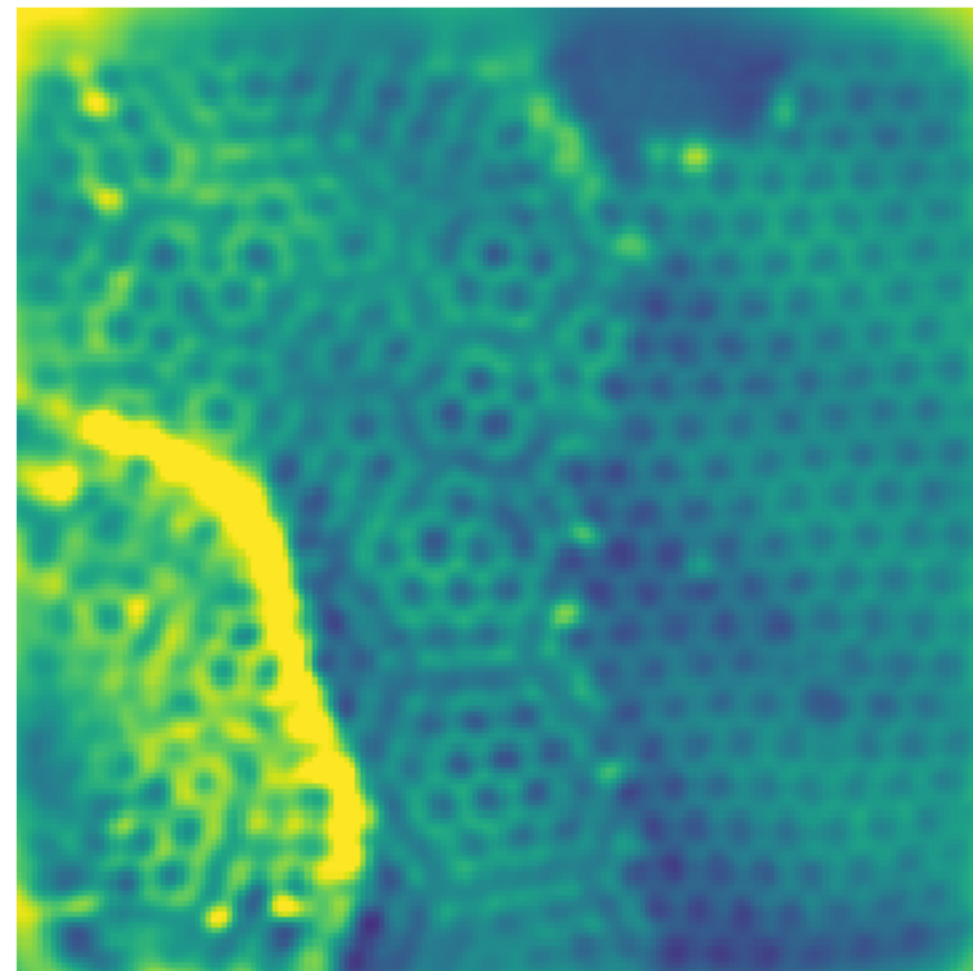
FFT(Probe) Amplitude

Example: Nonlinear CG

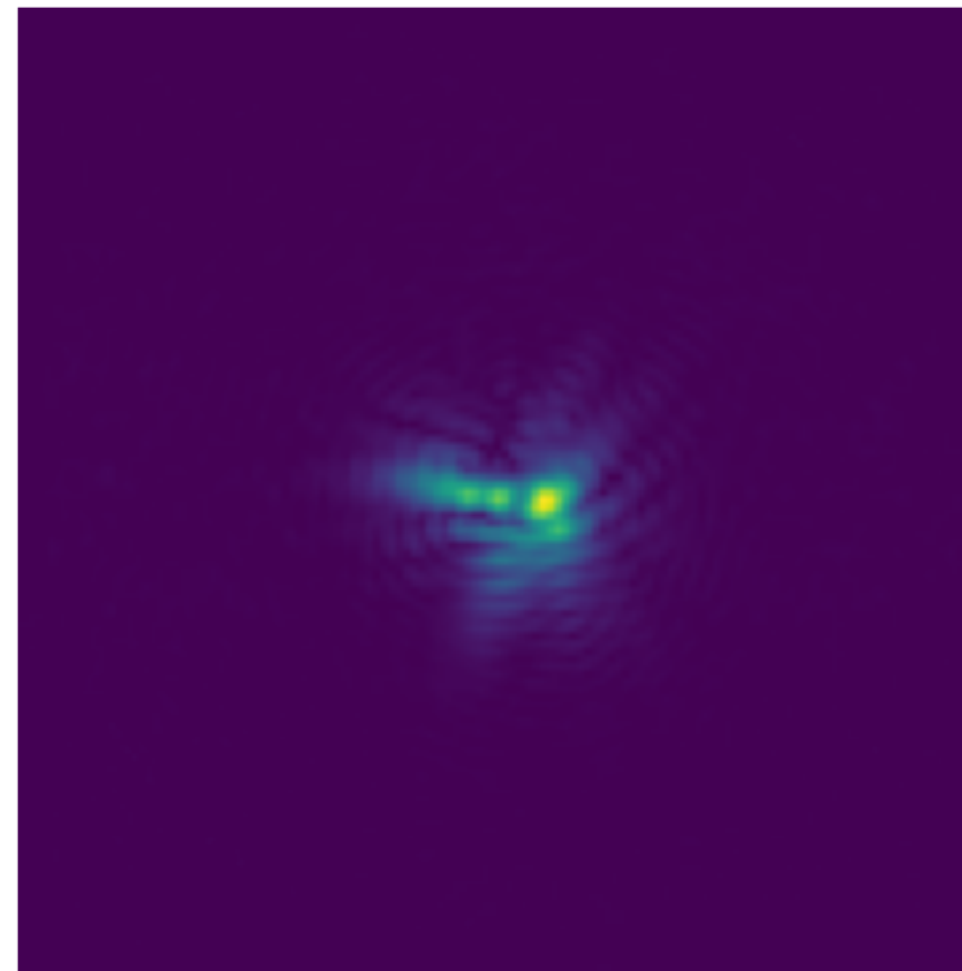
Graphene dataset courtesy of Chris Allen (ePSIC)



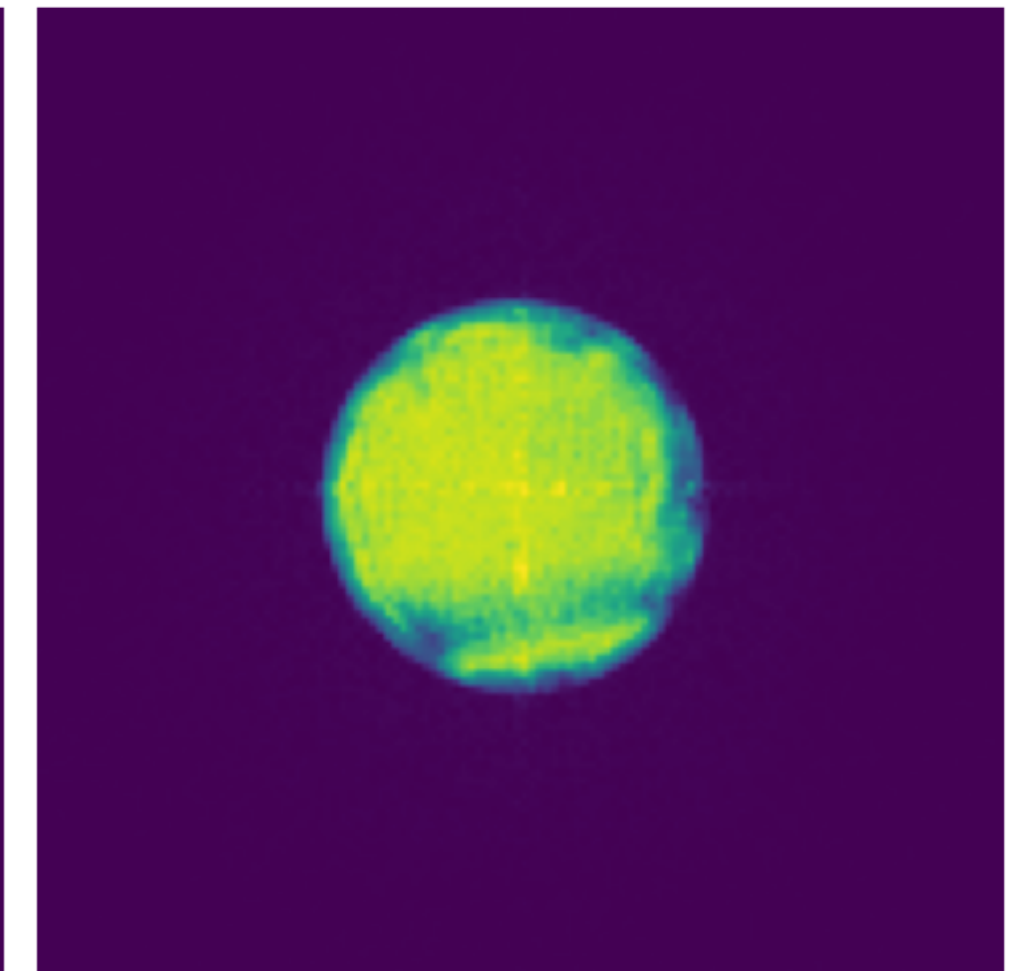
Object Amplitude



Object Phase



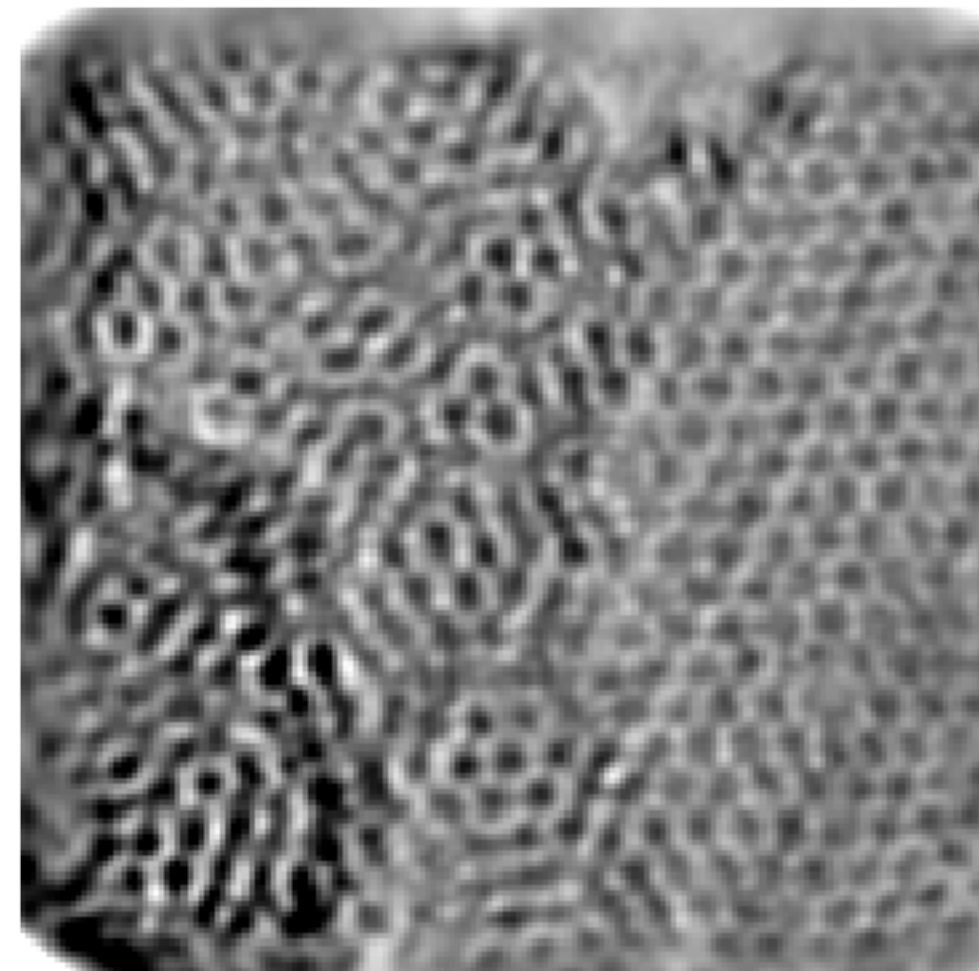
Probe Amplitude



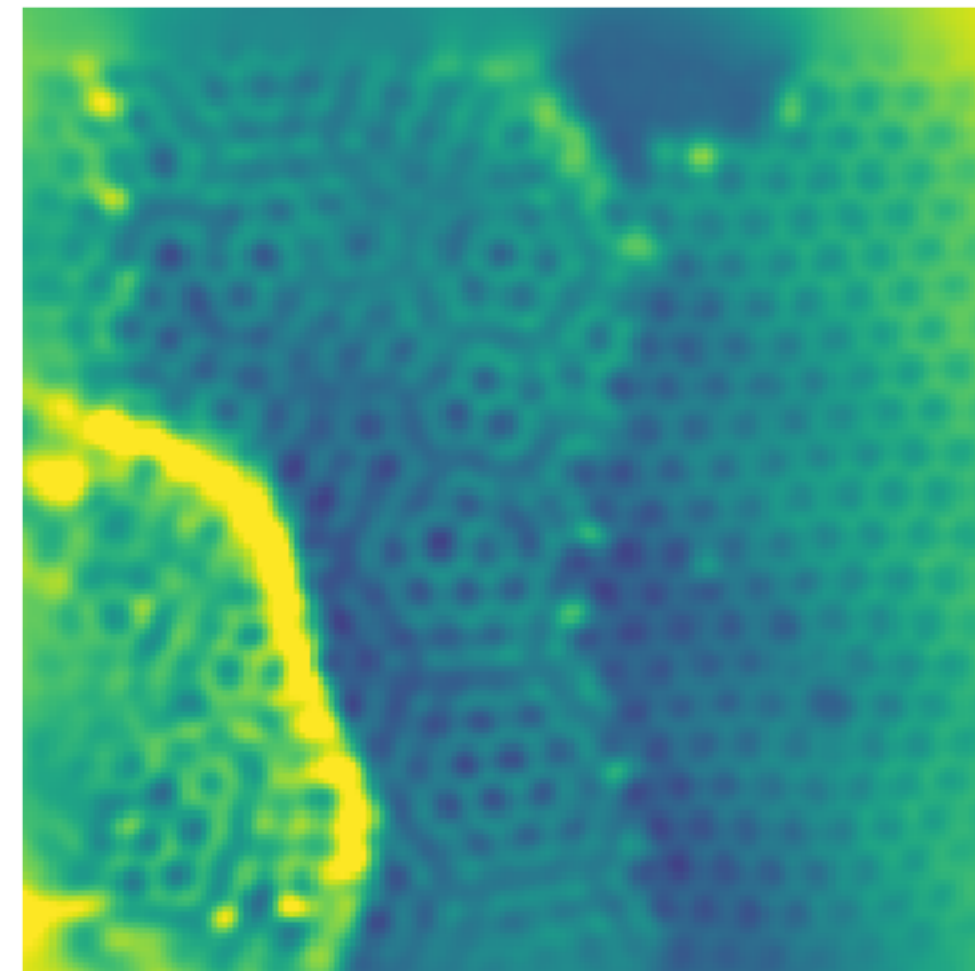
FFT(Probe) Amplitude

Example: L-BFGS

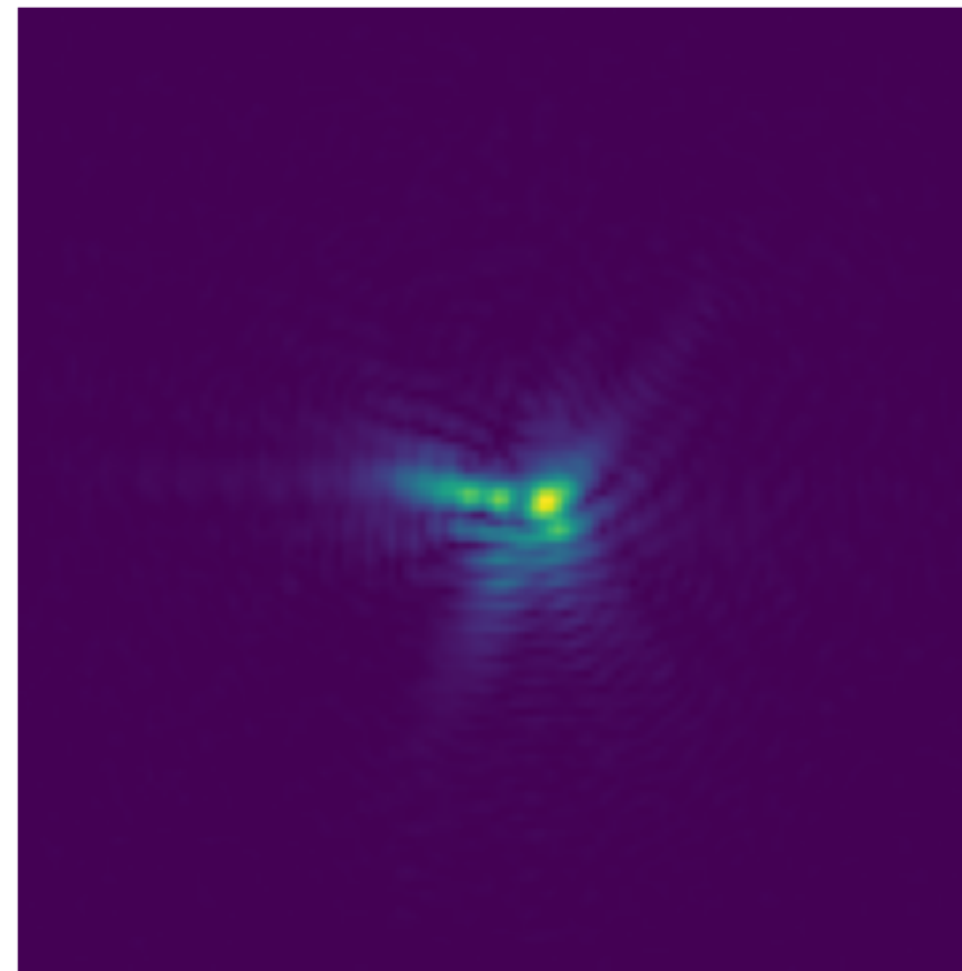
Graphene dataset courtesy of Chris Allen (ePSIC)



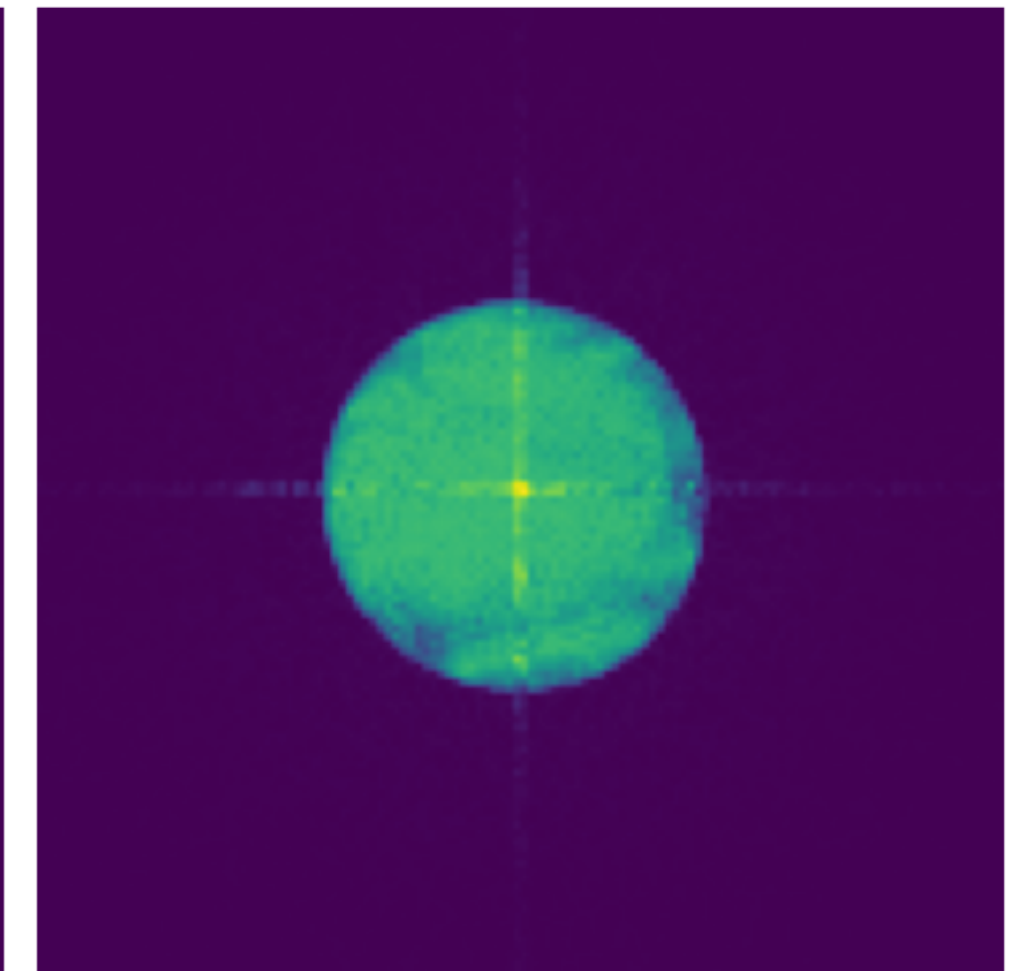
Object Amplitude



Object Phase

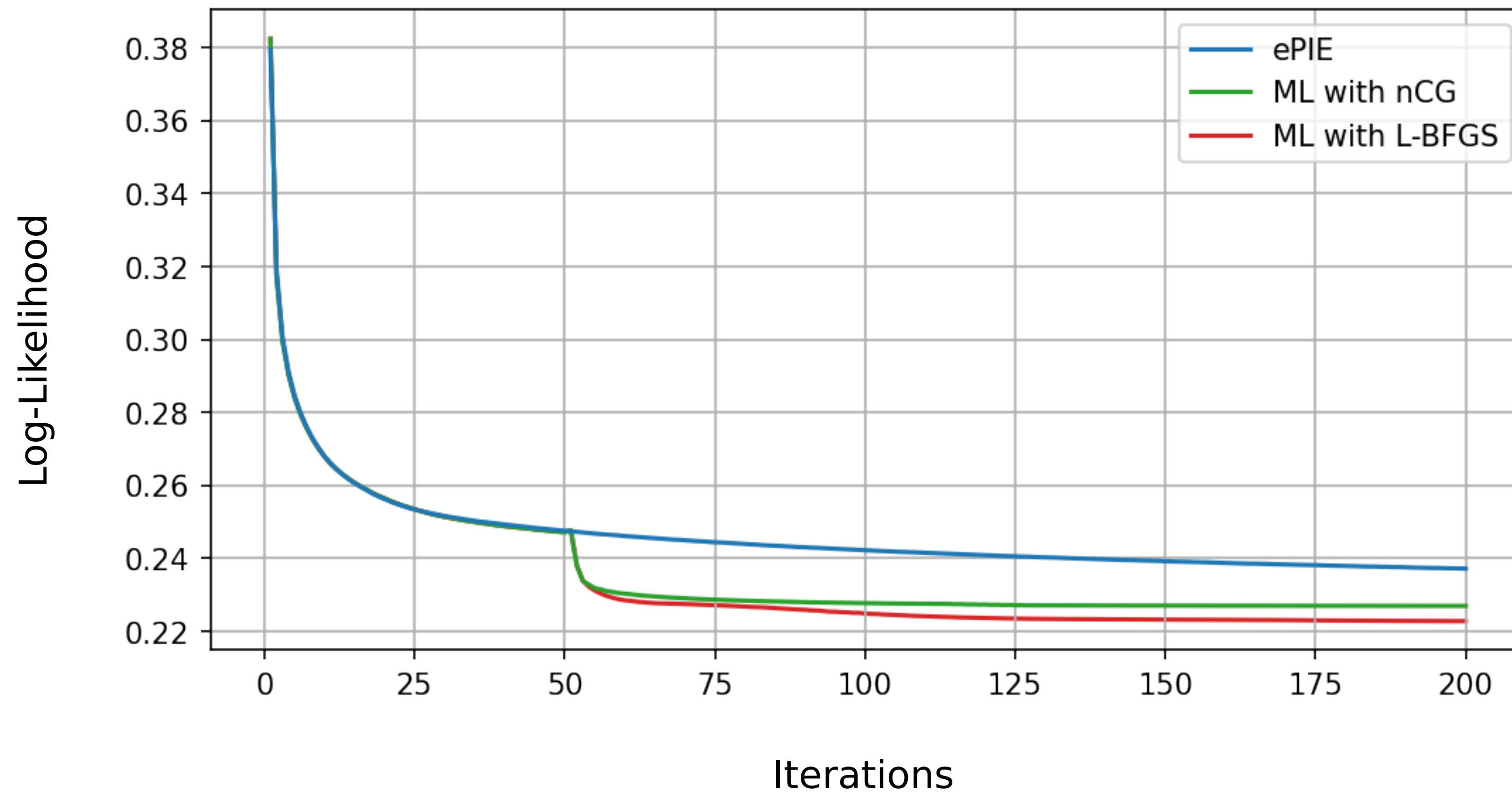


Probe Amplitude



FFT(Probe) Amplitude

Example: Log-Likelihood Error



Thank you! Questions?

References

- 📄 Fannjiang, A., & Strohmer, T. (2020). The numerics of phase retrieval. *Acta Numerica*, 29, 125-228.
- 📄 Thibault, P., & Guizar-Sicairos, M. (2012). Maximum-likelihood refinement for coherent diffractive imaging. *New Journal of Physics*, 14(6), 063004.
- 📄 Maiden, A., Johnson, D., & Li, P. (2017). Further improvements to the ptychographical iterative engine. *Optica*, 4(7), 736-745.
- 📄 Odstrčil, M., Menzel, A., & Guizar-Sicairos, M. (2018). Iterative least-squares solver for generalized maximum-likelihood ptychography. *Optics express*, 26(3), 3108-3123.
- 📄 Fowkes, J., Poon, T., Thibault, P., & Daurer, B. Reviewing gradient-based methods for ptychographic image reconstruction. *In preparation*.